Hyperfine interactions at lanthanide impurities in Fe

D. Torumba, V. Vanhoof, M. Rots, and S. Cottenier*
Instituut voor Kern- en Stralingsfysica and INPAC, Katholieke Universiteit Leuven, Celestijnenlaan 200 D, B-3001 Leuven, Belgium
(Received 8 May 2006; published 12 July 2006)

The magnetic hyperfine field and electric-field gradient at isolated lanthanide impurities in an Fe host lattice are calculated from first principles, allowing a qualitative and quantitative understanding of an experimental data set collected over the past 40 years. It is demonstrated that the common local density approximation leads to quantitatively and qualitatively wrong results, while the LDA+U method performs much better. In order to avoid pitfalls inherent to the LDA+U method, a combination of free ion calculations and "constrained density matrix" calculations is proposed and tested. Quantitative results for the exchange field and crystal field parameters are obtained (B_{exc}=+420 T, B_0^4=−1000 cm^{-1}, B_0^6=−800 cm^{-1}), showing in particular how crystal field effects influence the hyperfine fields for the lightest and heaviest lanthanides. The hyperfine fields are shown to be dominated by the 4*f* orbital contribution, with small corrections due to the spin dipolar and Fermi contact fields. The latter is found to be constant for all lanthanides, a feature that is understood by a modified version of the well-known core polarization mechanism for 3*d* hyperfine fields. Spin dipolar fields and electric-field gradients have apart from a 4*f* contribution a surprisingly strong contribution due to the completely filled lanthanide 5*p* orbitals—the mechanism behind this is explained. The lanthanide 4*f* spin moment is found to couple antiparallel to the magnetization of the Fe lattice, in agreement with the model of Campbell and Brooks. There is strong evidence for a delocalization-localization transition that is shifted from Ce to at least Pr and maybe further up to Sm. This shift is interpreted in terms of the effective pressure felt by lanthanides in Fe. Implications for resolving ambiguities in the determination of delocalization in pure lanthanide metals under pressure are discussed. For the localized lanthanides, Yb is shown to be divalent in this host lattice, while all others are trivalent (including Eu). The temperature dependence of the hyperfine fields is discussed as well.

DOI: 10.1103/PhysRevB.74.014409 PACS number(s): 75.20.Hr, 71.20.Eh, 75.25.+z, 76.80.+y

I. INTRODUCTION

A prototype problem in the field of nuclear condensed matter physics is to determine and understand the magnetic hyperfine field (HFF) at any of the elements of the periodic table, incorporated as a substitutional impurity in a simple ferromagnetic host such as bcc Fe. Understanding hyperfine fields forms a critical test for our understanding of condensed matter. Moreover, they provide a convenient tool for nuclear physicists to determine nuclear magnetic moments: two features that explain the decades of experimental[1] and theoretical[2,3] efforts that have been devoted to this problem. Today, the hyperfine fields of all elements as substitutional impurities in bcc Fe are well understood up to about Z=55.[4–8] For the heavier 5*d* impurities, sizable deviations between theory and experiment remain.[9] The hyperfine fields of very light impurities at interstitial sites in Fe have been calculated as well.[10,11] Lanthanide impurities in Fe are much less understood, both experimentally and theoretically. As far as experiment is concerned, it is hard to obtain *reliable* values for the lanthanide hyperfine fields (and also for their electric-field gradients; see below). This problem is illustrated by the rather desperate conclusion of Niesen in a still useful review[12] back in 1976: "*(…) if we cannot perform experiments that yield unambiguous results, we should better do no experiments at all*." On the theoretical side, no *ab initio* studies have been performed yet for lanthanide impurities in Fe (an approach using a model Hamiltonian is developed in Ref. 13). The reason for this lies in a known failure of the widely used local density approximation (LDA) within density functional theory (DFT): the LDA is not suitable to describe strong electron correlations.[14–17] As a result, the strongly correlated and mainly *localized* 4*f* states in lanthanides are rendered *itinerant* by the LDA. It can therefore be anticipated that for a lanthanide impurity in bcc Fe, the LDA is incapable of describing correctly the interaction between these localized and strongly correlated 4*f* electrons and the itinerant 3*d* states of the host material. This could be overcome by using the open-core formalism, an approach that has been used in the past with some success for lanthanides.[14,15,17] Although this treatment allows variation of the radial part of the wave function, the *f* electrons behave *qualitatively* as in free atoms, which is not entirely correct. An efficient and popular way to improve on the LDA failure without resorting to too atomiclike 4*f* behavior is to use the LDA+U method.[18–22] In LDA+U, the correlation absent in the LDA is reintroduced by an on-site Coulomb repulsion parameter *U*, to which an *a priori* value has to be assigned. The LDA+U method has been used in the recent past with considerable success (recent examples are Refs. 21 and 23–26 and many others), but it is not yet clear where the boundaries of its range of applicability are. In this work, we will examine how well LDA+U performs on a delicate quantity as the HFF.

An extra feature for lanthanide impurities in Fe that is absent for lighter impurities is the presence of a large electric-field gradient (EFG) at the lanthanide nucleus. At a site with cubic point symmetry—such as a substitutional site in bcc Fe—the EFG tensor must be necessarily zero. But the strong spin-orbit coupling for these heavy atoms lowers the symmetry to tetragonal, and as a result a large atomiclike EFG develops. The same happens for 5*d* impurities in Fe,[27–29] but there the spin-orbit coupling is weaker and the

TABLE I. Diagonal elements of the 7×7 $4f$-up density matrix for Tm in Fe (ferrimagnetic case), together with the orbital ($4f$), dipolar ($4f+5p$), and Fermi contributions to the total HFF (tesla). These diagonal elements give the occupation of each m orbital (between 0 and 1). The LDA result is compared with several LDA+U calculations, all with $U=0.6$ Ry. The LDA+U calculations differ only in the initial distribution of the f electrons over the different orbitals. In the second column, the total energy (in mRy/atom) of the LDA+U calculations is given, relative to case 2, which has the lowest energy (see text for discussion).

	ΔE	$m=-3$	$m=-2$	$m=-1$	$m=0$	$m=1$	$m=2$	$m=3$	B_{orb}	B_{dip}	B_{Fermi}	B_{tot}
LDA		0.98	0.95	0.96	0.71	0.86	0.52	0.54	−326	14	−41	−353
Case 1	1.7	1.00	0.99	0.99	0.99	0.99	0.01	0.01	−718	63	−41	−696
Case 2	0.0	0.99	0.99	0.99	0.99	0.01	0.99	0.01	−571	27	−41	−585
Case 3	1.6	0.99	0.99	0.99	0.02	0.99	0.99	0.01	−425	16	−42	−451
Case 4	3.2	0.99	0.99	0.02	0.99	0.99	0.99	0.01	−275	28	−42	−289
Case 5	8.9	1.00	0.04	0.99	0.99	0.99	0.99	0.01	−126	63	−42	−105

EFG is two orders of magnitude smaller than the values found in lanthanides. We have calculated and analyzed the EFG for lanthanides in iron and compare it with the sparse experimental data.

The goals of this work can be summarized as follows. On the physical side, we want to obtain better *quantitative* and *qualitative* insight into the magnetic hyperfine fields and electric-field gradients of lanthanide impurities in Fe. This should allow us to assess better the reliability of the existing experiments and to derive the underlying physical mechanism. On the technical side, we want to examine whether the range of applicability of the LDA+U method can be extended to problems as delicate and sensitive as magnetic and electric hyperfine interactions of heavy impurities in a transition metal host. It will be shown that in the course of this analysis unexpected new results and questions show up, such as the influence of the lanthanide $5p$ electrons (Secs. IV B and V B), the position of the delocalization-localization transition in this system (Secs. IV B and VI B), and the role of the crystal field (Secs. IV B 4 and V A).

II. COMPUTATIONAL DETAILS

All our calculations were performed within density functional theory,[30–32] using the augmented plane waves+local orbitals (APW+lo) method[32–34] as implemented in the WIEN2k package[35] to solve the scalar-relativistic Kohn-Sham equations. In the APW+lo method, the wave functions are expanded in spherical harmonics inside nonoverlapping atomic spheres of radius R_{MT} and in plane waves in the remaining space of the unit cell (=the interstitial region). For the Fe atoms a R_{MT} value of 2.20 a.u. was chosen, while for the lanthanide impurity we used $R_{\text{MT}}=2.45$ a.u. The maximum ℓ for the expansion of the wave function in spherical harmonics inside the spheres was taken to be $\ell_{\text{max}}=10$. The plane wave expansion of the wave function in the interstitial region was made up to $K_{\text{max}}=7.5/R_{\text{MT}}^{\text{min}}=3.41$ a.u.$^{-1}$, and the charge density was Fourier expanded up to $G_{\text{max}}=16\sqrt{Ry}$.

The lattice constant of Fe was fixed at the experimental value of 2.87 Å. In order to reproduce the situation of an isolated impurity in bulk Fe, we used the supercell approach with a $2\times2\times2$ supercell where one iron atom was replaced by a lanthanide atom. The neighboring Fe atoms are displaced by the presence of this impurity, as was documented before for lighter impurities in Fe.[3,7,8] We took this effect into account in an average way by relaxing the nearest neighbors for Eu as an impurity (which is in the middle of the lanthanide series) and kept the same relaxation fixed for all other lanthanides. The Eu-Fe distance was 2.60 Å which is an increase of 0.11 Å with respect to the Fe-Fe distance and which is almost identical to the distance between $5p$ impurities and their Fe neighbors.[8] It was tested for another lanthanide (Er) that there was only a marginal difference of less than 1 T between the HFF obtained with the Eu-Fe distance and the correct Er-Fe distance (2.58 Å). A test for an extended supercell of 32 atoms was also performed. We relaxed the first four nearest neighbors. The Eu-Fe distance hardly changed (2.63 Å) and the Fermi contribution to the hyperfine field changed with 5 T. For the sampling of the Brillouin zone (BZ) of the $2\times2\times2$ supercell we took 75 special **k** points in the irreducible part of the BZ, which corresponds to a $10\times10\times10$ mesh.

As exchange-correlation functional, the local density approximation[36] was used. For the LDA+U method, the "around the mean field" (AMF) scheme of Czyżyk and Sawatzky[19] was used. A few cases were duplicated with the fully localized limit[20] (FLL) version of LDA+U and this turned out not to change qualitatively the results (for instance, the order of the five cases in Table I was the same). The choice of the U and J parameters is discussed in detail in Sec. IV B. In the LDA+U method the total energy is a functional not only of the density, but also of the density matrices, defined as

$$\left\langle \Psi \left| a^{\dagger}\left(m_l', \frac{1}{2}\right)\left(m_l, \frac{1}{2}\right)\right| \Psi \right\rangle \text{ (up-up)},$$

$$\left\langle \Psi \left| a^{\dagger}\left(m_l', -\frac{1}{2}\right)\left(m_l, -\frac{1}{2}\right)\right| \Psi \right\rangle \text{ (dn-dn)},$$

$$\left\langle \Psi \left| a^{\dagger}\left(m_l', \frac{1}{2}\right)\left(m_l, -\frac{1}{2}\right)\right| \Psi \right\rangle \text{ (up-dn)},$$

for spin-up, spin-down, and up-down cross terms.

For some of our calculations the density matrices will be constrained to an *a priori* value; in others they will freely

evolve throughout the self consistent cycle. Sometimes the effect of the cross term will be neglected. Details will be given in the appropriate sections. The LDA+U calculations were performed using the orbital package of WIEN2k. In this implementation a few approximations are made. The first assumption is that relativistic mass enhancement can be neglected (for orbital properties only—in the regular self-consistency cycle scalar-relativistic effects are included). This approximation is harmless for the $3d$ atoms, but it may have an influence on lanthanides and actinides.[37] Second, it is assumed that the nuclear spin is parallel with the electron spin and with the electron orbital moment. This might be dangerous for atoms with large orbital moments (as some lanthanides), where the orbital moment could be strongly pinned to a crystal direction. Another assumption is that contributions from the interstitial region and contributions non-diagonal in l can be neglected. Finally it is assumed that $\langle \hat{O}(r)\hat{O}(\vec{l},\vec{s})\rangle = \langle \hat{O}(r)\rangle\langle \hat{O}(\vec{l},\vec{s})\rangle$ [where $\hat{O}(r,\vec{l},\vec{s})$ is either the orbital moment, orbital HFF, or dipolar HFF operator]. Free atoms were simulated by a supercell containing only one lanthanide and vacuum otherwise, leading to a separation of 9.4 Å between two "neighboring" lanthanides. For free ion calculations, this cell was charged. All the other parameters were chosen exactly the same as in the calculations for lanthanides in Fe.

Relativistic local orbitals (RLO's) for the lanthanide 5p states were added to the basis set, because it is known that for actinides this allows one to reduce the basis set size needed for the second variational step[38] (=lower $E_{\mathrm{cut}}^{\mathrm{SO}}$). Limitations in the implementation prevent one from obtaining correct EFG's and dipolar HFF's when RLO's are used. Therefore, whenever such information was needed, the calculations were repeated without RLO's. This never had a large influence on the obtained values, however.

The interaction between a lanthanide ion and its solid-state environment can be phe-nomenologically modelled by the following single-ion Hamiltonian:[14]

$$\hat{H} = \lambda \hat{L}\cdot\hat{S} + 2\mu_B \hat{B}_{exc}\cdot\hat{S} + \sum_{k,q} B_q^k C_q^k. \qquad (1)$$

The three interactions that contribute to the total energy of such a system are the spin-orbit, exchange, and crystal field interactions. In the above equation λ is the spin-orbit constant, B_{exc} is the exchange field that acts on the $4f$ spin (Sec. IV B 1), and the sum represents the crystal potential (Sec. IV B 4). Spin-orbit coupling is the dominant interaction, while the crystal field interaction is the weakest[14] ($E_{so} > E_{exc} > E_{cf}$), except for the edges of the lanthanide series where the exchange and crystal field interactions have the same order of magnitude. Spin-orbit (SO) coupling was taken into account in all the calculations by a second-variational-step scheme,[39] using a cutoff energy $E_{\mathrm{cut}}^{\mathrm{SO}}$ =3.0 Ry. We will show below how we determined the values of the exchange field (Sec. IV B 1) and the crystal field parameters (Sec. IV B 4), such that all parameters in Eq. (1) will be quantitatively known.

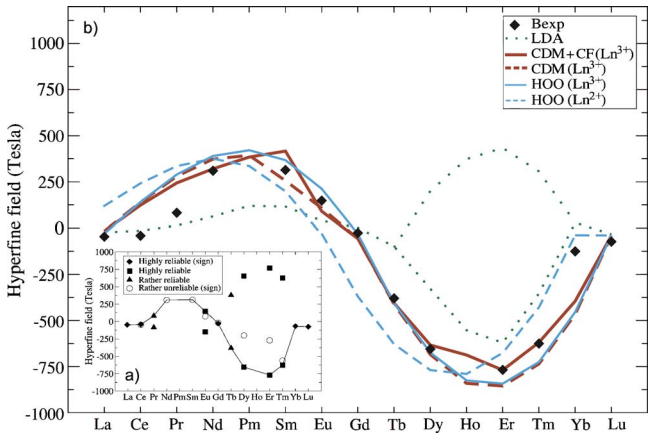

FIG. 1. (Color online) Comparison between experiment and several types of calculations for the magnetic hyperfine field of lanthanides in Fe. Diamonds: most probable experimental data points [this is the solid line from (a)]. Gray (green) dotted line: LDA results for the ferrimagnetic orientation (Campbell-Brooks orientation) and for the ferromagnetic orientation when this one has the lowest energy. Solid lines and dashed lines: LDA+U calculations for trivalent and divalent lanthanides (see text). Inset picture: experimental data set for the magnetic hyperfine fields of lanthanides in Fe. If the sign of the HFF is not measured, the data point is plotted at both positive and negative values. A distinction is made (see text) between highly reliable data for which the sign is measured (diamond), highly reliable data without sign measurement (square), less reliable data without sign (triangle), and data that are rather unreliable for the magnitude of the HFF but reliable for the sign (circle). For references and values, see text. The line connects the most likely values for all lanthanides. If multiple measurements with the same reliability were available, only one of them is given. More data can be found in the compilation of Rao (Ref. 1).

III. EXPERIMENTAL DATA SET

A. Magnetic hyperfine fields

Let us first have a look at the experimental data set for the HFF [Fig. 1(a)]. Only in four cases are the magnitude of the HFF *and* its sign known with high reliability [the sign of the HFF indicates whether the field is parallel (+) or antiparallel (−) with respect to the magnetization of the Fe host lattice]. These cases are La [−47(1) T],[40] Ce [−41(2) T],[41] and Lu [−73.12(36) T],[42] for which nuclear magnetic resonance on oriented nuclei (NMR/ON) has been performed, and Yb [−125(8) T],[43] on which time-dependent perturbed angular correlation spectroscopy (TDPAC) has been applied. The latter technique has also been used for Gd,[44] albeit on a recoil-implanted sample which is not necessarily clean. The value of −26(8) T obtained in this way agrees well with an in principle reliable Mössbauer measurement of −37 T, which is unfortunately not very well documented.[45] Three time-integrated perturbed angular correlation (IPAC) measurements are available for Gd as well—IPAC is a method that is rather unreliable and can merely be used to determine the sign and an order of magnitude. They yield −20(5) T,[46] −18(9) T,[47] and −7 T.[48] A HFF of −30(10) T can therefore be assigned to Gd in Fe in a reliable way. In four other cases the magnitude of the HFF but not its sign has been measured

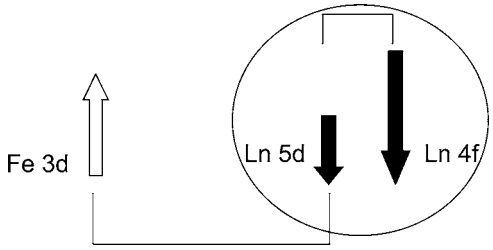

FIG. 2. Schematic summary of the model of Campbell and Brooks, illustrating the ferromagnetic intraatomic 4*f*-5*d* coupling and the ferrimagnetic interatomic coupling between Fe 3*d* and Ln 5*d* moments (see text).

with an accurate method as Mössbauer spectroscopy (MS): Eu [148.2(9) T],[49,50] Dy [610(7) T],[51] Er [768(13) T],[52] and Tm (671 T).[12] For Pr[53] and Tb,[54] the magnitude but not the sign has been measured with low-temperature nuclear orientation (LTNO). This nonresonant technique provides data that are less accurate than the previous ones, although they still are reasonably reliable. Finally, in the case of Ce,[55] Nd,[46] Sm,[56] Eu,[46] Gd,[47] Dy,[47] Er,[46] and Tm[57] IPAC experiments have been reported, from which only the sign information can be reasonably trusted [see, e.g., the agreement with other experiments in Fig. 1(a) and Ref. 1]. Due to the latter sign information, the HFF of the light lanthanides is guessed to be positive, while for the heavy lanthanides it is negative. The line in Fig. 1(a) summarizes the most likely interpretation of this data set.

Figure 1(a) can be understood in terms of Hund's rules and the model of Campbell and Brooks. Based on heuristic arguments (Ref. 58) and first-principles calculations (Ref. 59), Campbell and Brooks showed that the *interatomic* exchange interaction between a transition metal 3*d* spin moment and a lanthanide 5*d* spin moment is ferrimagnetic (Fig. 2). The lanthanide 4*f* moment is localized at the lanthanide site and cannot directly interact with its transition metal neighbors, but it has a ferromagnetic *intra-atomic* exchange interaction with the lanthanide 5*d* moment. The result is a net ferrimagnetic coupling between the lanthanide 4*f* moment and the transition metal 3*d* moment—except for Lu and divalent Yb, where the 4*f* moment is zero (Fig. 2). According to Hund's third rule, the lanthanide orbital moment is antiparallel to the lanthanide spin moment for the seven lightest lanthanides and parallel to it for the seven heaviest lanthanides. The dominant contribution to the HFF is the orbital HFF (see Sec. IV A and Fig. 3), which is parallel to the orbital moment. Therefore, one expects the total HFF to be parallel to the Fe magnetization (and hence positive) for the light lanthanides and antiparallel (negative) for the heavy ones, as is seen indeed in Fig. 1(a).

B. Electric field gradient

Only few experimental data on the main component V_{zz} of the electric-field gradient tensor for lanthanides in Fe are available (Fig. 4). For Eu, Dy, Er, and Tm, Mössbauer measurements[12,50] were done. Some attention is needed for Eu, which is reported to have $V_{zz}=0$ in Ref. 12, based on

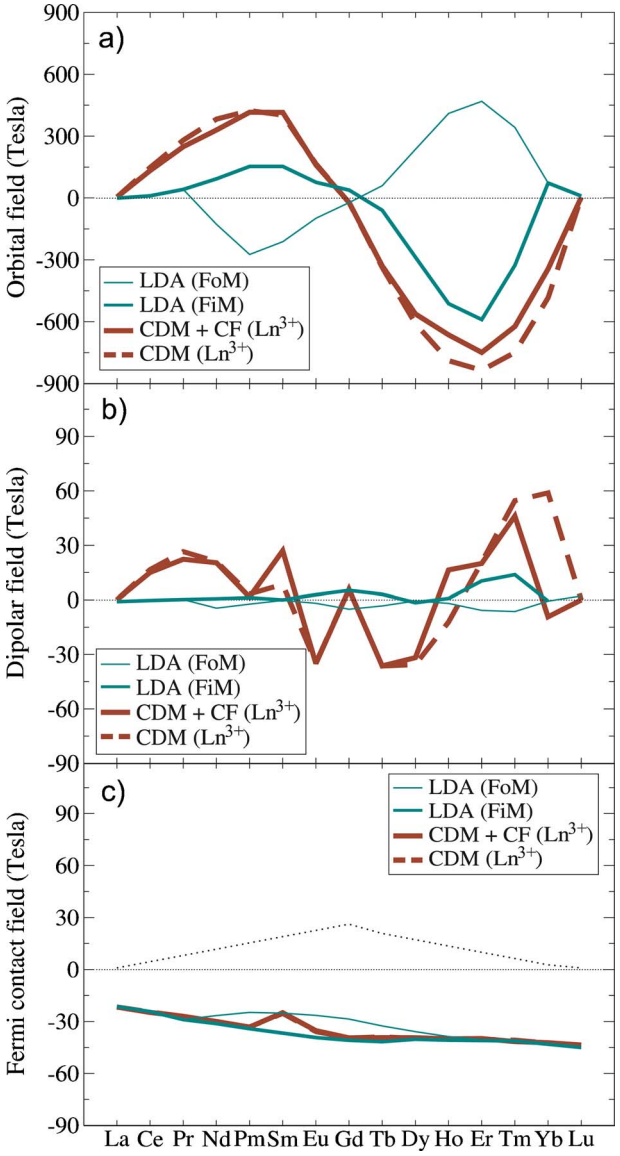

FIG. 3. (Color online) Thin gray (green) line: the LDA ferromagnetic solution (FoM). Thick gray (green) line: the LDA ferrimagnetic solution (FiM). Black (red) lines: the contributions to the HFF obtained with the CDM method without considering the crystal field interaction (dashed line) and with crystal field effects taken into account (solid line). Mind the scale, which is 10 times larger in (a) compared to (b) and (c). (a) Orbital contribution to the HFF at the lanthanide site due to 4*f* electrons. (b) Dipolar contribution to the HFF. (c) Fermi contribution. The CF has no effect on the Fermi contribution; therefore, the two black (red) lines coincide. The dotted line represents the Fermi HFF for the free lanthanide ions. The Fermi HFF obtained with CDM is indistinguishable from the one obtained with LDA. The total HFF is the sum of (a), (b), and (c), and is almost undistinguishable from (a).

^{151}Eu Mössbauer spectroscopy from Ref. 49. Niesen and Ofer, however, have later shown[50] by ^{153}Eu Mössbauer spectroscopy that $V_{zz}=-11.110^{21}$ V/m^2. For Ce in Fe the quadrupole coupling constant (which contains the product between V_{zz} and the quadrupole moment Q) has been determined by ^{141}Ce NMR (Ref. 60) to be almost zero. The quadrupole moment for ^{141}Ce is not known, but assuming a

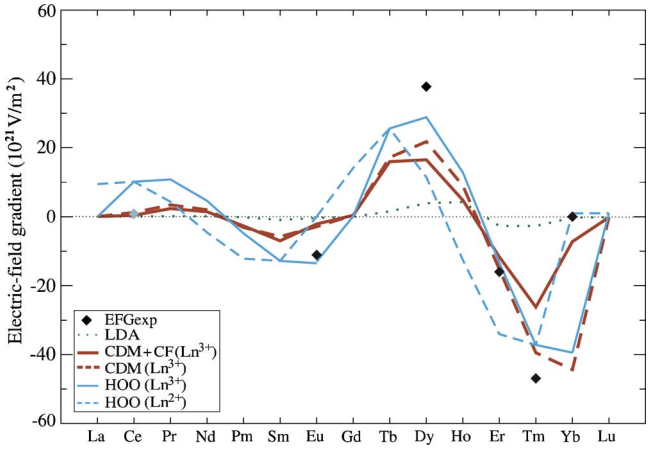

FIG. 4. (Color online) V_{zz} for lanthanides in Fe. Symbols: experimental data (Refs. 12, 43, 50, and 60) (see text). The gray symbol for Ce indicates that this value is a—rather safe—guess (see text). Dotted line: LDA results. Solid and dashed lines: LDA+U values for trivalent and divalent lanthanides (see text).

typical value of 1 b leads to a V_{zz} that is practically zero (gray symbol in Fig. 4). The zero V_{zz} for Yb is not explicitly mentioned in the literature, but can be inferred from Fig. 1 in Ref. 43, which shows a purely magnetic interaction.

IV. CALCULATIONS

A. LDA calculations

As a first step, we calculate the magnetic HFF with the common LDA. This will provide us with a data set to which we can later compare the possible improvement by LDA+U, and it allows us to introduce some peculiarities that will play a role in all later calculations as well. As is usual with this type of methods, our calculations involve an iterative procedure ("self-consistent field" procedure) that yields in the end a possible state of the calculated system, which is not necessarily the desired ground state: in the space of possible solutions, this self-consistent field procedure finds a *local* minimum, but not necessarily the *global* minimum. The local minimum that is obtained depends to some degree on the starting configuration that was initially chosen. This behavior is prominently present for lanthanides in Fe. If the spin moment of the lanthanide initially is put parallel to the Fe spin moment, then this orientation is maintained throughout the iterative procedure (except for La, Ce, and Pr, where the moment always spontaneously turns to an antiparallel orientation). We call this from now on the ferromagnetic solution. With an initially antiparallel configuration, an antiparallel (or ferrimagnetic) solution is obtained. If the lanthanide was given initially no spin moment, then a solution with a spin moment that is much reduced compared to the two preceding solutions was found. In order to decide which of those is the ground state, one has to look at the total energy of each solution. The total energy of the case with reduced moment was much higher than the others, and we will not consider it further. The energy differences between the other two solutions are given in Fig. 5(a). For all lanthanides up to Tb, the

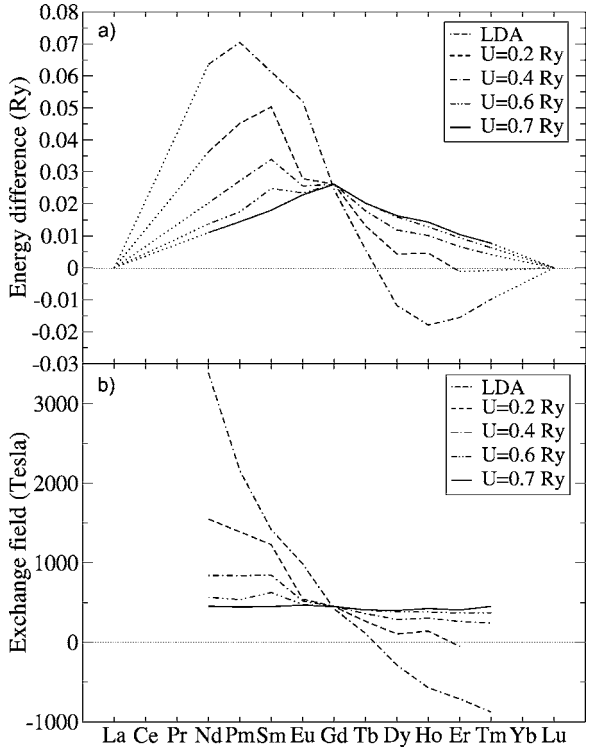

FIG. 5. (a) Energy difference between the situations with the lanthanide 4*f* spin moment ferromagnetically aligned with the Fe 3*d* moment and with the 4*f* moment ferrimagnetically aligned ($E_{\mathrm{FoM}}-E_{\mathrm{FiM}}$). If this energy difference is positive, the ferrimagnetic situation has the lowest energy. Energy differences for LDA are compared with energy differences for LDA+U with progressively larger U. The LDA result is equivalent to $U=0.0$ Ry. (b) Exchange field obtained from the energy differences from (a) as a function of U [$B_{exc}=(E_{\mathrm{FoM}}-E_{\mathrm{FiM}})/(|\mu_{4f}^{\mathrm{FoM}}|+|\mu_{4f}^{\mathrm{FiM}}|)$].

ferrimagnetic solution has the lower energy. Starting with Dy, the ferromagnetic solution becomes the ground state.

In Fig. 3, the different contributions to the magnetic HFF are given for both types of solutions. A HFF is a magnetic field at the position of the nucleus, and it is built mainly from three contributions: the spin dipolar field, the Fermi contact field, and the orbital field. The spin dipolar field is generated by the spin moments of the electrons surrounding the nucleus. For cubic point symmetry, this contribution vanishes. The Fermi contact field[61] is of dipolar nature as well, but is due to the penetration of *s* electrons into the nucleus. It does not vanish for cubic symmetry, and it is the dominant (and almost only) contribution for impurities up to $Z=55$ in Fe. The orbital field stems from the electric charge of the electron that orbits the nucleus, and it vanishes for cubic symmetry. As Fig. 3 shows, the dipolar field does not exceed a few tesla, while the Fermi contact field lies between −20 T and −40 T (WIEN2k versions prior to January 2006 yield the wrong sign for the dipolar HFF). The orbital field is the dominant contribution and can reach almost ±600 T. At first sight, one would expect a zero orbital and dipolar field for a substitutional impurity in Fe, as the point symmetry is cubic. The reason why this is not the case for lanthanides is the same one that allows the presence of a large EFG (Sec. I). The oscillatory behavior of the orbital moment reflects

Hund's third rule: the orbital moment is antiparallel (parallel) to the spin moment in the first (second) half of the lanthanide series. Because the orbital field is parallel to the orbital moment, it will for the ferrimagnetic solution be positive in the first half of the series and negative in the second half (and vice versa for the ferromagnetic solution).

According to the LDA total energies, we have to accept the ferrimagnetic solution as the ground state up to Tb and the ferromagnetic solution starting from Dy. This leads to positive HFF's for almost all lanthanides [Fig. 1(b)], which is in contradiction with the current interpretation of the experimental data set and with the model of Campbell and Brooks. We will demonstrate in Sec. IV B that this is a new, clear example of a failure of the LDA. Even if we would select the ferrimagnetic solution throughout (as the Campbell-Brooks model suggests), then still the quantitative agreement with the experimental HFF's is rather poor [Fig. 1(b)].

B. LDA+U calculations

1. Exchange field

Using and interpreting LDA+U calculations brings some complications that are absent for LDA. First, LDA+U schemes are not fully *ab initio*: they involve an on-site Coulomb repulsion parameter U and an on-site exchange interaction constant J that have to be chosen *a priori* for every orbital with strong correlations. In our case we have to choose one U and one J for the f states of the lanthanide impurity. In line with the strategy adopted for the relaxation (Sec. II), we strive for reasonable overall agreement and do not focus on agreement for individual cases too much. Therefore we take the same U and J for all lanthanides.

How do we choose their values? In order to answer this question we examine the energy difference between the ferromagnetic and the ferrimagnetic case for qualitatively the same type of solution [as we will show soon, there will be many different types of solution for LDA+U—the criterion to decide whether there is a *qualitative* difference between two solutions or not is provided by the $4f$ density matrix: in qualitatively similar cases, the occupation of the 14 m orbitals (=the diagonal elements of the two spin-polarized 7×7 density matrices) should be more or less identical]. The result is shown in Fig. 5, for four different values of U: 0.2, 0.4, 0.6, and 0.7 Ry. The alignment of the Ln $4f$ moment with respect to the Fe $3d$ moment (mediated by the Ln $5d$ moment; see Fig. 2) results in an energy which is represented by the second term of the Hamiltonian from Eq. (1):

$$E_{exc} = 2\mu_B \vec{B}_{exc} \cdot \vec{S}^{4f}, \tag{2}$$

where B_{exc} is the exchange field. Therefore, the energy difference between the ferromagnetic and ferrimagnetic solutions will be proportional to the $4f$ spin moment:

$$\Delta E_{exc} = 4\mu_B B_{exc} S^{4f}. \tag{3}$$

The magnitude of the $4f$ spin moment increases linearly from zero (in the case of La) to $7\mu_B$ for Gd, then decreases to zero again for Lu. As can be observed in Fig. 5(a), this proportionality with the $4f$ spin magnetic moment is obtained for a value of $U=0.7$ Ry. We also expect a constant exchange field for all lanthanides. This method of determining the exchange field from the total energy difference between the ground state and a state with reversed $4f$ spin moment was introduced by Liebs *et al.*[62] (for more examples see Ref. 14 and references therein). In Fig. 5(b) we observe that we obtain indeed a constant field of 420 T for all the lanthanides for $U=0.7$ Ry. Therefore, this is the U we have to use in our calculations. Looking at other calculations[18,63] and experiments,[64,65] $U=0.7$ Ry is indeed a reasonable choice. The value of J is usually an order of magnitude smaller, and it does not affect the results as much as U does. Therefore we take J as 10% of U. Moreover, if we look at the sign of the energy difference between the ferromagnetic and the ferrimagnetic case [Fig. 5(a)], we observe that the use of a $U>0.2$ Ry makes the ferrimagnetic case more stable, for all lanthanides. This brings the sign of the HFF in agreement with experiment and with the model of Campbell and Brooks. We conclude that LDA+U describes the effective d-f exchange interaction much better than the LDA does and that the LDA is qualitatively wrong in this respect.

Another—second—complication with LDA+U is the fact that there are now much more local minima in the space of solutions than for the LDA (see beginning of Sec. IV A) and a calculation gets easily trapped in one of them. This problem is illustrated in Table I, where the diagonal elements of the $4f$-up density matrix are given for various ferrimagnetic solutions for Tm in Fe. The five electrons can be distributed in different ways over the seven orbitals, and always a converged solution can be obtained (it is the absence of this orbital freedom in the LDA that avoids many of those local minima there). The HFF field can be very different for all cases. In the second column, the total energy of these five solutions is given, relative to the case with the lowest energy ("case 2"). The same total energy criterium we used before for the LDA (Sec. IV A) now should lead to the conclusion that "case 2" is the ground state for Tm in Fe (LDA+U at fixed U is a variational method,[66,67] such that the ground state corresponds to the lowest LDA+U total energy). However, one would expect a Hund's rule state ("case 1") as ground state for the localized $4f$ electrons (we will see later that indeed this is the case), such that it is a bit cumbersome that "case 2" has the lowest energy. Two possible explanations for this observation are the following: (1) Different spin states may have different values of U and a particular value of U is suitable for one spin state, but not for the others. Perhaps all five cases in Table I need their own U, such that total energy comparisons become invalid anyway. (2) Perhaps the incompletely compensated self-interaction in the energy functional for the highly correlated f states spoils the accuracy of the total energy,[68] such that unphysical conclusions might indeed show up. This point is not completely understood.

Having determined the value of the exchange field in Eq. (1), we now address the problem of multiple solutions. This will result in a first set of predictions for the ground-state values of the HFF's in the ferrimagnetic case.

2. First method: Constrained density matrix calculations

Our first approach of finding the true ground state amid the multitude of different solutions is based on the fact that

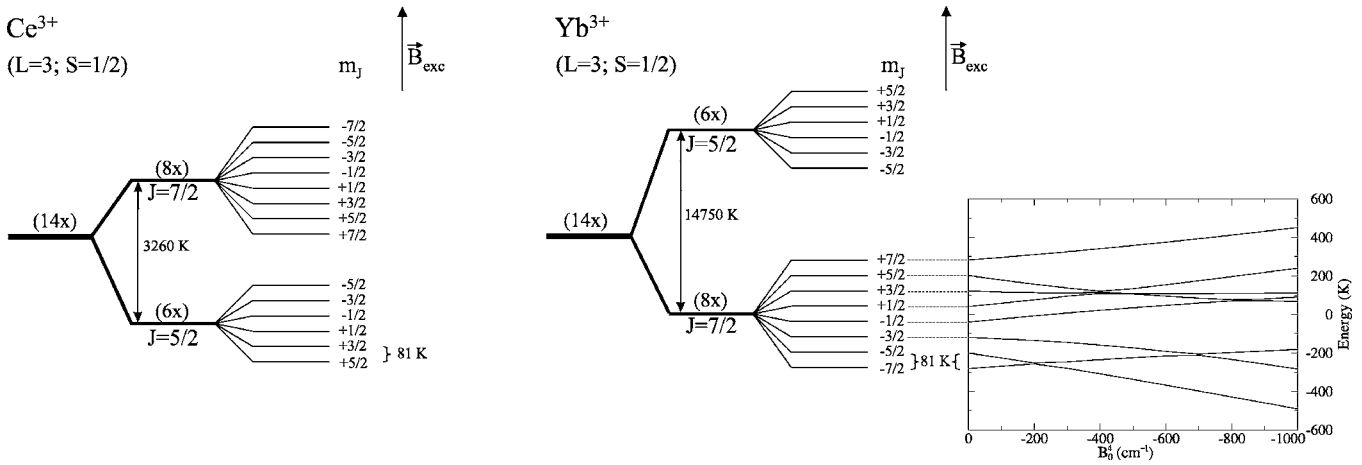

FIG. 6. The exchange-field-split ground-state multiplets of Ce^{3+} and Yb^{3+} ions and the influence of the crystal field on the energy levels ($B_0^6=0$). The sizes of the various energy splittings are also indicated (in kelvin).

the f electrons of the lanthanides are only weakly influenced by the surrounding Fe environment—the ground state should therefore not deviate too much from a free lanthanide ion. Therefore, we calculate the spin density matrices corresponding to the exchange-split ground-state multiplet of the free lanthanide ion, and using these density matrices we perform LDA+U calculations for the case of lanthanides in Fe. In a first step we will neglect the crystal field interaction, which will have an influence only at the edges of the lanthanide series (we come back to that point in Sec. IV B 4). Calculating the spin density matrices corresponding to the ground state of the lanthanides ions was done by the LANTHANIDE code, developed by Edvardsson and Åberg.[69] This atomic program provides the energy levels of equivalent f electrons and the corresponding spin density matrices for the ground-state multiplet under the influence of an external (not exchange) field for lanthanide or actinide trivalent ions. Many-body interactions are included by configuration interaction. Applying an external field instead of an exchange field gives the same ground state when S and J are parallel (the exchange field acts on the $4f$ spin moment while the external magnetic field couples to the total magnetic moment). In the first half of the series (from Ce to Sm) we therefore have to switch the sign of the external field in order to act as an exchange field (because S and J are antiparallel). In order to get the same size of splitting by the external field as would have been caused by an exchange field, the magnitude of the external field has to be adjusted [$\Delta E_{ext} \sim g_J$ while $\Delta E_{exc} \sim (1-g_J)$]. The correct exchange-split ground-state multiplet for the trivalent lanthanide ions was calculated both analytically[70] and by using the MCPHASE program[71] (see Fig. 6). Using the LANTHANIDE program with an external field acting as an exchange field and ignoring, for the moment, the crystal field interaction, we have calculated the spin-up, spin-down, and cross-term density matrices of the f electrons. The parameters needed for density matrix calculations were taken from Ref. 72. For all the lanthanides the spin-up and -down matrices are diagonal. Analyzing these matrices (Table II), one can observe that we have fractional occupation of the m orbitals in the first half of the lanthanide series, while for heavier lanthanides the occupation is integer or almost integer. The cross-term matrix has nonzero elements only above the diagonal and only if the occupation of the corresponding m orbitals is noninteger (Table III). Subsequently we performed LDA+U calculations for every lanthanide in Fe, *keeping the previously obtained density matrices fixed*. Or, in other words, a self-consistent solution was obtained under the constraint that the density matrices should have their exchange-split free ion values. The fixed density matrices serve as a tool to introduce many-body effects from the free ion calculation into the mean-field LDA+U calculation. The results obtained using this approach are plotted in Fig. 1 [black (red) dashed line] and will be discussed in Sec. V A.

For obvious reasons, we will further refer to this approach as *constrained density matrix* (CDM) calculations. Because the density matrices are fixed, all freedom for obtaining multiple solutions with LDA+U has been removed. By construction, the single solution that is found is close to the free ion ground state (properly taking into account the magnetic influence of the environment) and is therefore believed to be a good approximation of the ground state in the solid as well.

TABLE II. Spin-up, spin-down, and cross-term density matrices for Pr^{3+} and Dy^{3+} ions, obtained by the LANTHANIDE program for $B_{exc}=420$ T.

	Spin up							Spin down						
	$m=-3$	$m=-2$	$m=-1$	$m=0$	$m=1$	$m=2$	$m=3$	$m=-3$	$m=-2$	$m=-1$	$m=0$	$m=1$	$m=2$	$m=3$
Pr^{3+}	0.00	0.00	0.00	0.01	0.16	0.02	0.05	0.00	0.00	0.00	0.00	0.04	0.79	0.92
Dy^{3+}	1.00	1.00	0.02	0.02	0.02	0.01	0.00	1.00	1.00	1.00	0.98	0.98	0.98	0.99

TABLE III. Cross-term density matrix for Pr^{3+} and Dy^{3+} ions, obtained by the LANTHANIDE program for B_{exc}=420 T.

(m,m')	$(-3,-2)$	$(-2,-1)$	$(-1,0)$	$(0,1)$	$(1,2)$	$(2,3)$
Pr^{3+}	0.00	0.00	0.00	−0.02	−0.35	−0.14
Dy^{3+}	0.00	0.00	−0.14	−0.13	−0.13	−0.10

In Sec. IV B 4 we will go one step further and introduce crystal field effects. That will require a lot of LDA+U calculations, more than is feasible with such a rather time-consuming *ab initio* method (typically one day per calculation). Therefore we will in the next section first develop an approximate but very fast method that will allow us to obtain HFF and EFG for any given density matrix within seconds.

3. Second method: Hyperfine fields by orbital occupation

We can turn the annoying freedom of having several ways to occupy the m orbitals into an advantage by determining the *individual contribution* of each m orbital to, e.g., the orbital field (this method will not be exact for all lanthanides; see later). This can be done by first calculating the orbital HFF for several different ferrimagnetic solutions, as is given as an example for Tm in Table I (without constraining the density matrices, in contrast to the CDM method). Then a system of linear equations is set up, with as seven variables x_m the orbital HFF of each of the seven m orbitals. The occupations of each of these orbitals (or the diagonal elements of the density matrix from Table I) are the coefficients. The occupation found in the calculation should give the calculated orbital field, as is illustrated here for "case 1" in Table I:

$$1.00x_{-3} + 0.99x_{-2} + 0.99x_{-1} + 0.99x_0 + 0.99x_1 + 0.01x_2 + 0.01x_3 = -718.$$

This system of equations can be supplemented by other equations expressing some general truths (the orbital field with all seven m orbitals filled is zero; the contribution by $+m$ is opposite to the one by $-m$), such that the system becomes overdetermined. Each subset of seven independent equations should give the same x_m, which indeed they do. Because this method will be used only for integer occupation (see Sec. V), in these calculations we ignore the cross terms (for integer occupation the cross terms are zero). Having found the x_m for a particular lanthanide, we can now immediately get the orbital hyperfine field of that lanthanide for a given occupation of the m orbitals (=for a given diagonal of the density matrix) by summing the products of x_m and the occupation number. We call this method *hyperfine fields by occupation of orbitals* (HOO). It requires a limited number of calibrating LDA+U calculations, but once the x_m are found the hyperfine field for any occupation of the orbitals can be immediately obtained. As a way to check the reliability of the HOO method, a detailed analysis is given in Table IV for the Tm with its $m=+3$ and $m=+2$ orbitals unoccupied. This is the same configuration as "case 1" in Table I, and a very similar HFF is found indeed. The CDM method for the Tm ground state leads to B_{orb}=−748 T and B_{dip}=55 T, again very similar numbers. The HOO method is especially accurate for the second half of the lanthanide series, where the density matrix elements are close to being integers (0 or 1) and up-down cross-term matrix elements are consequently almost zero (cross-term contributions to the HFF are absent in HOO). In that sense, HOO can be understood as the limit of integer occupation of the m orbitals.

TABLE IV. Contributions to B_{orb}, B_{dip}, and V_{zz} for Tm in Fe in the Hund's rules ground state, using the information from Figs. 7–9.

Tm	B_{orb} (T)	B_{dip} (T)	V_{zz} (10^{21} V/m^2)
$4f$-up	−745	49	−76.2
$4f$-down	−1	1	0.9
$5p$-up	−84	−10	16.1
$5p$-down	83	13	21.2
$6p$-up	10	0	−0.7
$6p$-down	−8	0	0.1
Sum	−745	53	−38.6

This HOO approach was used for ten elements from the lanthanides series (Ce, Nd, Pm, Sm, Tb, Dy, Ho, Er, Tm, and Yb), not only for the orbital HFF but also for the dipolar HFF (Figs. 7 and 8). A general analysis of the properties of orbital and dipolar HFF for lanthanides will be given now, based on Figs. 7 and 8. The total HFF and EFG for lanthanides in Fe will be discussed in Secs. V A and V B. The dominant contribution to the orbital HFF is due to the $4f$ electrons, as one could expect [Figs. 7(a) and 7(b)]. Orbitals with opposite m quantum number yield opposite orbital hyperfine fields. The latter can be understood as follows (see also Table V): in orbitals with opposite m, the electrons move in opposite directions, because opposite m (z component of the orbital angular momentum) mean that the angular momenta of those orbitals have different orientations. Hence, the orbital fields will be opposite as well. As a function of Z, the contribution due to each m orbital increases. A linear fit is possible (solid line). In order to verify whether this is accidental or not, we did the same calculations for free lanthanide atoms and free lanthanide 3^+ ions. For the free ions, almost the same perfect linear correlation was found as for the solid (dotted lines in Fig. 7). For free neutral atoms, the fields were slightly larger (at most 10% for the orbital field and 5% for the dipolar field). Additional to this large $4f$ contribution, there is also a $5p$ contribution to the orbital HFF [Figs. 7(c)–7(e)]. The up and down contributions are quite large (40–90 T), but they cancel each other, yielding a negligible (<3 T) total contribution for the $5p$-orbital HFF. This $5p$ contribution to the orbital HFF does not depend on the f configuration. Taking Dy as an example—two electrons in the unfilled spin channel—the total $5p$ orbital field will be −2 T (72 T for $5p$-up, −74 T for $5p$-down), irrespective whether these two electrons are, e.g., in the $m=+3$ and $m=+2$ or in the $m=-1$ and $m=0$ orbitals. This will be different for dipolar hyperfine fields and for the electric-field gradient. Looking separately to the $5p$-up and -down contributions, one can see that they do not vanish for La ($4f$ empty) and Lu ($4f$ full) and that they increase with Z. Moreover, we ob-

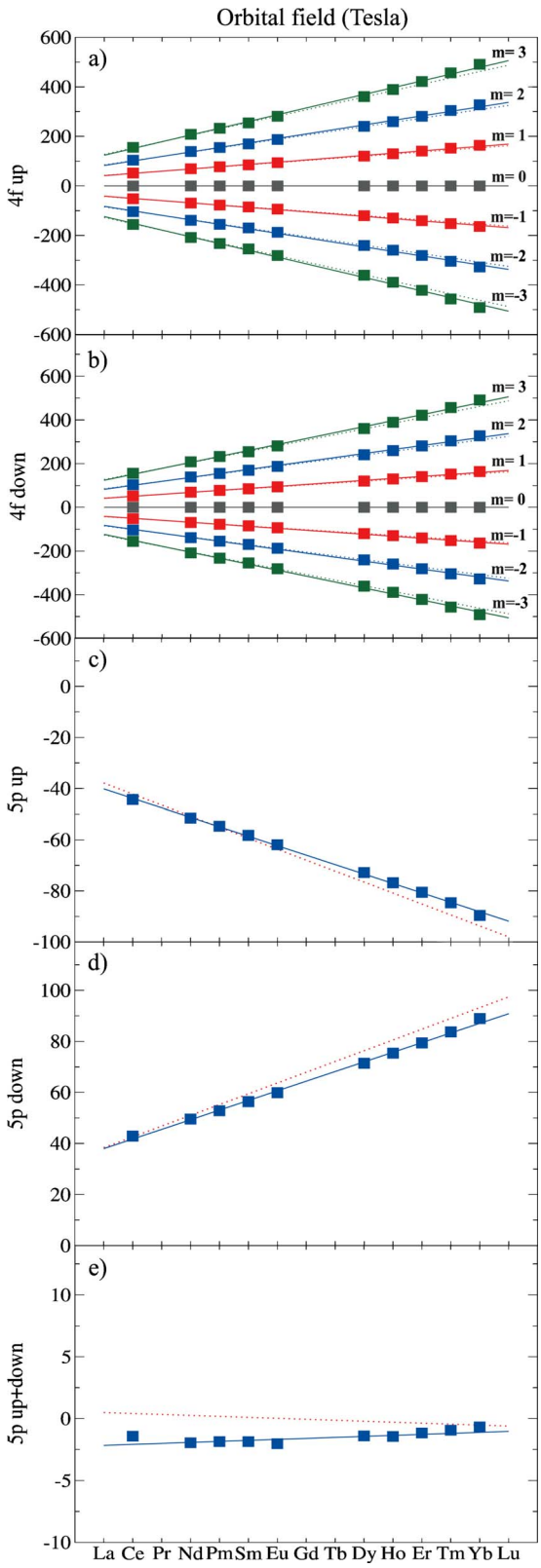

FIG. 7. (Color online) Contribution of each m orbital to the (a) 4f-up, (b) 4f-down orbital HFF and the contribution of the (c) 5p-up, (d) 5p-down, (e) 5p up+down electrons to the orbital HFF of a lanthanide in Fe. Data points: results from calculations for lanthanides in Fe. Solid lines: linear fit through these data points. Dotted lines: linear fit through a complete set of calculations for free lanthanide ions.

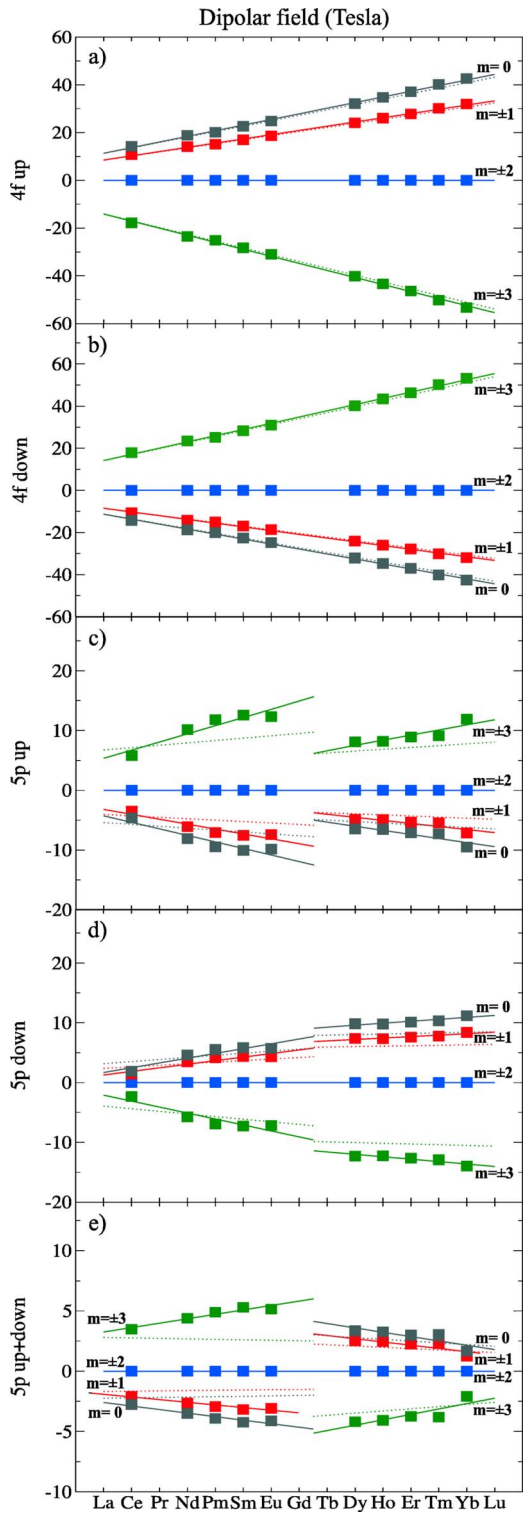

FIG. 8. (Color online) Contribution of each m orbital to the (a) 4f-up, (b) 4f-down dipolar HFF and the induced (c) 5p-up, (d) 5p-down, (e) 5p up+down contributions to the dipolar HFF of a lanthanide in Fe (the 5p-up and 5p-dn contributions correspond to the FiM solutions; for the FoM orientation the pictures for 5p up and down have to be interchanged). Data points: results from calculations for lanthanides in Fe. Solid lines: linear fit through these data points. Dotted lines: linear fit through a complete set of calculations for free lanthanide ions.

TABLE V. Overview whether μ_{orb}, B_{orb}, B_{dip}, and V_{zz} depend on the shape of the $4f$ orbital (given by the absolute value of m), the direction of motion of the electron in that orbital (given by the sign of m), and whether they depend on the charge or on the spin of the $4f$ electron in a given m orbital.

	μ_{orb}	B_{orb}	B_{dip}	V_{zz}
Shape of orbital	Yes	Yes	Yes	Yes
Direction of motion	Yes	Yes	No	No
Charge or spin	Charge	Charge	Spin	Charge

served that this contribution disappears if the SO coupling is switched off. Therefore we can conclude that these $5p$ contributions are due to an intrinsic p effect, induced by the SO coupling on the p electrons which breaks the cubic symmetry. Finally there is also a contribution from the valence $6p$ electrons, also induced by the SO coupling, but this contribution is really small and can be neglected.

For the dipolar HFF as well, the $4f$ contribution remains the dominant one [Figs. 8(a) and 8(b)], but it is one order of magnitude smaller than the orbital HFF. The systematics are different from the orbital moment and orbital HFF as well [Figs. 8(a) and 8(b) and Table V]. First of all, the dipolar HFF does not depend on the direction of motion of an electron, such that $\pm m$ orbitals yield the same dipolar HFF. Second, B_{dip} depends explicitly on the electron spin, such that an electron with opposite spin in the same m orbital yields an oppositie field. Furthermore, we can observe from Figs. 8(c)–8(e) that the $5p$ contributions to B_{dip} depend on the $4f$ occupation. If we take again Dy as an example and put the two electrons in the +3 and +2 orbitals (spin up), we get an induced $5p$ contribution of 4 T (−8 T for $5p$-up and 12 T for $5p$-down), while this is −3 T (4 T for $5p$-up and −7 T for $5p$-down) if the two electrons are in the +1 and −2 orbitals (spin up). Such a $4f$ dependence was not present for B_{orb} (and also not for the orbital moment). In Sec. V B we will see that also for the EFG there is such an explicit $4f$ dependence, and we will be able to explain this by the radial dependences, which are $1/r$ for μ_{orb} and B_{orb} and $1/r^3$ for B_{dip} and V_{zz}. Another observation from Fig. 8 is that the induced $5p$ contributions behave differently in the first and second halves of the lanthanide series. This suggests a spin-dependent interaction. In the first half of the series the unfilled f band is the down band (Figs. 7–9 are made in the assumption that first spin down is filled, then spin up—if not, then the pictures for $5p$-up and -down have to be interchanged). The $5p$-up contribution is large; the $5p$-down is smaller. In the second half the unfilled f band is the up band. Now the $5p$-up contribution is small and $5p$-down larger. We will show later (Sec. V B) that $4f$ and $5p$ electrons try to avoid each other, and as Figs. 8 and 9 show this avoidance is different for identical or different spins: we see here a manifestation of the Pauli principle. The $6p$ contribution remains negligible also for the dipolar HFF.

4. Crystal field

In this section we will discuss the last term of the model Hamiltonian [Eq. (1)], the crystal field term. The crystal field (CF) Hamiltonian describes the interaction of the crystal potential with the $4f$ electrons. Following Wybourne's formalism,[73] the crystal field Hamiltonian can be written as

$$H_{CF} = \sum_{k,q} B_q^k C_q^k, \tag{4}$$

where C_q^k are the components of a spherical tensor of rank k and B_q^k are the so-called crystal field parameters. The summation involves all the f electrons of the ion of interest. The first term in the expansion ($k=q=0$) is spherically symmetric and can be ignored as far as the crystal field splittings of the levels are concerned. On the other hand, if the f electrons are involved, the only nonzero terms in the expansion are those with $k \leqslant 6$. Furthermore, all terms with odd k vanish for configurations containing equivalent electrons. The remaining crystal field parameters can be zero or not depending on the site symmetry. Considering all these things together with the fact that the lanthanides in Fe are situated on a site with cubic symmetry the CF Hamiltonian in our case can be written as

$$H_{CF} = B_0^4 C_0^4 + B_4^4 (C_{-4}^4 + C_4^4) + B_0^6 C_0^6 + B_4^6 (C_{-4}^6 + C_4^6). \tag{5}$$

Because the crystal potential has to be invariant under the twofold rotation axis of a cube, the parameters can be related in the following way:

$$B_4^4 = \sqrt{\frac{5}{14}} B_0^4, \tag{6}$$

$$B_4^6 = -\sqrt{\frac{7}{2}} B_0^6. \tag{7}$$

Finally, the CF Hamiltonian for our problem is

$$H_{CF} = B_0^4 \left[C_0^4 + \sqrt{\frac{5}{14}} (C_{-4}^4 + C_4^4) \right] + B_0^6 \left[C_0^6 - \sqrt{\frac{7}{2}} (C_{-4}^6 + C_4^6) \right]. \tag{8}$$

The problem one has to solve now is to find the remaining two CF parameters B_0^4 and B_0^6 for the lanthanide in Fe situation. In order to find these parameters we have used the LANTHANIDE program to obtain the spin density matrices for different B_0^4 and B_0^6 (keeping the exchange field to fixed to the previously found value). The B_0^4 was varied between -2000 cm^{-1} and $+1000$ cm^{-1} while B_0^6 covers the interval from -1000 cm^{-1} to $+1000$ cm^{-1}. Both CF parameters were varied in steps of 100 units, leading to 651 different sets of crystal field parameters for every lanthanide. For each density matrix obtained, the total magnetic hyperfine field was determined using the fast HOO method described in Sec. IV B 3 (the large number of cases to be examined is the reason why it was necessary to have something as this fast HOO method). We have applied this algorithm for the four lanthanides from the second half for which we have reliable experimental hyperfine fields: Tb, Dy, Er, and Tm (Fig. 10). Only the lanthanides from the second half were chosen because we noticed already that the HOO method is valid only for integer occupation, which is the case in the second half of

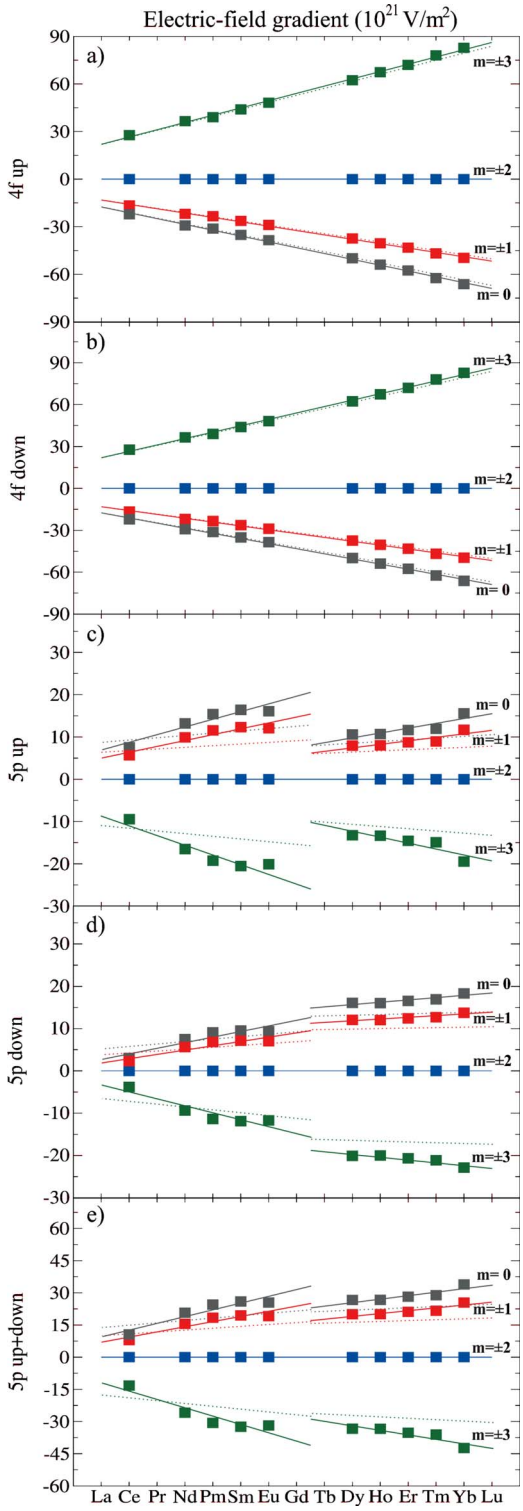

FIG. 9. (Color online) Contribution of each m orbital to the (a) 4f-up, (b) 4f-down to the total V_{zz} and the induced (c) 5p-up, (d) 5p-down, (e) 5p up+down to the total V_{zz} of a lanthanide in Fe (the 5p-up and 5p-dn contributions correspond to the FiM solutions; for the FoM orientation the pictures for 5p up and down have to be interchanged). Data points: results from calculations for lanthanides in Fe. Solid lines: linear fit through these data points. Dotted lines: linear fit through a complete set of calculations for free lanthanide ions.

the lanthanides series (see also Sec. V). Yb was not included because it occurs often in divalent configuration and its valency is something we want to determine (see also Sec. V). Figure 10 shows the deviation between the HOO-HFF and the experimental HFF for Dy and Er, as a function of CF parameters. There is one case (for $B_0^4=-1000$ cm^{-1} and $B_0^6=-800$ cm^{-1}) where this deviation is small for *both* elements. Similar plots for Tb and Tm (not shown) have a minimum at exactly the same point, such that we conclude that these particular values of B_0^4 and B_0^6 indeed represent the crystal field that is felt by all lanthanides in Fe. Now we generate the spin density matrices (up, down, and cross term) for all lanthanides using $B_{exc}=420$ T, $B_0^4=-1000$ cm^{-1}, and $B_0^6=-800$ cm^{-1} and apply the CDM method (Sec. IV B 2) to get the hyperfine field and the electric-field gradient. The results are given in Figs. 1 and 4, and the contributions to the hyperfine field are plotted in Fig. 3 ("CDM+CF"). A discussion will be given in Secs. IV A and V B. In Table VI we can see the density matrices obtained including the CF parameters for two ions: Pr^{3+} and Dy^{3+}. If we compare these spin density matrices with the ones obtained without considering CF effects (Tables II and III), we notice that although some additional off-diagonal terms appear, the f-electron occupation does not change qualitatively, which implies that CF interaction plays only a secondary role.

V. DISCUSSION

A. Magnetic hyperfine field

In Fig. 3 we can see the three contributions to the hyperfine field calculated using the methods described above. The dominant contribution is the orbital one, which stems from the 4f electrons of the lanthanides. There is also a small 5p contribution, which can be neglected. The dipolar hyperfine field is 10 times smaller than the orbital HFF and again it comes mainly from the f electrons. While these two contributions are different for each lanthanide and are much increased in the LDA+U calculations, the Fermi field is constant through the series and is unaffected by LDA+U (the crystal field, however, has some effect for Sm and to a lesser extent for Eu). The Fermi contribution is the sum of a core contribution (1s–4s electrons) and a valence contribution (5s and 6s). For magnetic impurities, the phenomenon of *exchange polarization* is largely responsible for determining the value of the Fermi field.[37] Exchange polarization is the name for a polarizing effect on the s electrons due to their exchange interaction with a polarized (=moment-carrying) d or f shell.[74] This interaction is schematically depicted in Fig. 11, for the case of free ions. In the case of 3d elements the 1s and 2s electrons lie spatially inside the 3d electrons, while the 4s electrons are outside the 3d shell. Therefore, the up-down polarization for 1s and 2s will be opposite to the polarization for 4s, leading to a Fermi HFF opposite to the 3d moment for 1s and 2s electrons and a 4s contribution that tends to cancel 1s and 2s.[74,75] The 2s and 4s contributions are larger than the 1s contribution, because these orbitals are spatially closest to the 3d and therefore have a stronger exchange interaction. The 3s contribution will be smaller and can be neglected in a qualitative discussion, due to overlap of

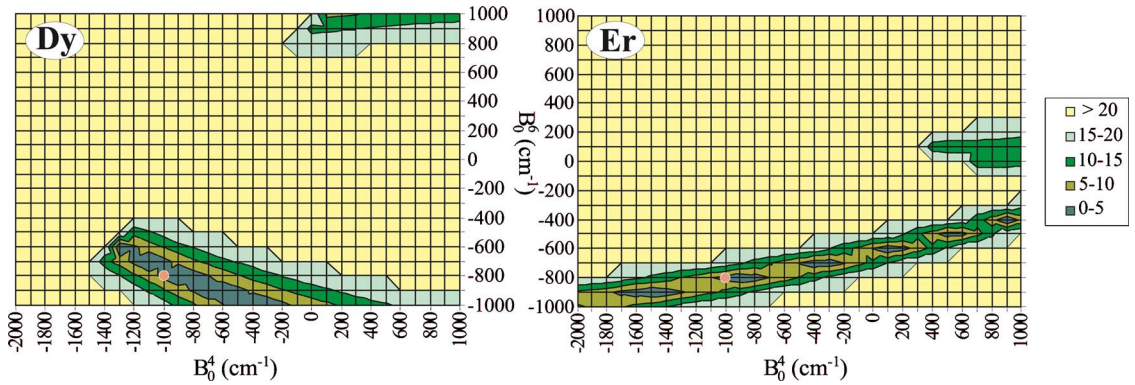

FIG. 10. (Color online) The deviation of the total HFF from experiment (in tesla) as a function of the CF parameters for Dy (left) and Er (right). The grey (red) circles indicate the values we have chosen for the CF parameters.

the 3*s* and 3*d* shells which leads to competing and mutually canceling tendencies. The mechanism as just described does not work in the case of 4*d* ions, because the radial distribution function of 4*d* electrons has one radial node that separates the largest outer component from the inner component. As a result the 4*d* shell will overlap with most of the *s* shells that are responsible for the contact HFF, leading to an undecided situation as for the 3*d* and 3*s*. On the other hand, in the case of 4*f* ions we have a similar situation as for 3*d* ions: there are no nodes in the 4*f* radial distribution function, and therefore the same exchange polarization mechanism is valid. Assuming a positive 4*f* moment, this will induce a negative Fermi HFF for the 1*s*, 2*s*, and 3*s* electrons and a positive HFF for the 5*s* and 6*s* electrons (see Table VII for an illustration, which is, however, for a negative moment and not for free ions). The overlap between 4*f* and 4*s* shell is similar with the 3*d*-3*s* and reduces the 4*s* contribution to a small value with either sign. The main contributions to the Fermi HFF will be 3*s* and 5*s*. By making the sum of all these individual contributions we get a total Fermi HFF proportional with the 4*f* moment [dotted line in Fig. 3(c)]. The difference between a free lanthanide ion and the case of lan-

TABLE VI. Spin-up, spin-down, and cross-term density matrices for Pr^{3+} and Dy^{3+} ions, obtained by the LANTHANIDE program for B_{exc}=420 T and the crystal field parameters B_0^4=−1000 cm^{-1} and B_0^6=−800 cm^{-1}.

		Pr^{3+}							Dy^{3+}						
Spin	*m*	−3	−2	−1	0	1	2	3	−3	−2	−1	0	1	2	3
Up	−3	0.01	0.00	0.00	0.00	0.00	0.00	0.00	0.95	0.00	0.00	0.00	0.15	0.00	0.00
	−2	0.00	0.04	0.00	0.00	0.00	0.02	0.00	0.00	0.97	0.00	0.00	0.00	−0.08	0.00
	−1	0.00	0.00	0.03	0.00	0.00	0.00	0.04	0.00	0.00	0.06	0.00	0.00	0.00	0.00
	0	0.00	0.00	0.00	0.02	0.00	0.00	0.00	0.00	0.00	0.00	0.08	0.00	0.00	0.00
	1	0.00	0.00	0.00	0.00	0.17	0.00	0.00	0.15	0.00	0.00	0.00	0.07	0.00	0.00
	2	0.00	0.02	0.00	0.00	0.00	0.03	0.00	0.00	−0.08	0.00	0.00	0.00	0.03	0.00
	3	0.00	0.00	0.04	0.00	0.00	0.00	0.05	0.00	0.00	0.00	0.00	0.00	0.00	0.01
Down	−3	0.00	0.00	0.00	0.00	0.00	0.00	0.00	0.99	0.00	0.00	0.00	−0.01	0.00	0.00
	−2	0.00	0.02	0.00	0.00	0.00	−0.09	0.00	0.00	0.98	0.00	0.00	0.00	0.01	0.00
	−1	0.00	0.00	0.07	0.00	0.00	0.00	0.22	0.00	0.00	0.98	0.00	0.00	0.00	0.00
	0	0.00	0.00	0.00	0.02	0.00	0.00	0.00	0.00	0.00	0.00	0.97	0.00	0.00	0.00
	1	0.00	0.00	0.00	0.00	0.08	0.00	0.00	−0.01	0.00	0.00	0.00	0.96	0.00	0.00
	2	0.00	−0.09	0.00	0.00	0.00	0.70	0.00	0.00	0.01	0.00	0.00	0.00	0.97	0.00
	3	0.00	0.00	0.22	0.00	0.00	0.00	0.77	0.00	0.00	0.00	0.00	0.00	0.00	0.98
Updn	−3	0.00	−0.01	0.00	0.00	0.00	0.01	0.00	0.00	−0.03	0.00	0.00	0.00	0.02	0.00
	−2	0.00	0.00	−0.05	0.00	0.00	0.00	−0.15	0.00	0.00	−0.01	0.00	0.00	0.00	−0.01
	−1	0.00	0.00	0.00	−0.02	0.00	0.00	0.00	0.00	0.00	0.00	−0.15	0.00	0.00	0.00
	0	0.00	0.00	0.00	0.00	−0.04	0.00	0.00	−0.08	0.00	0.00	0.00	−0.14	0.00	0.00
	1	0.00	0.04	0.00	0.00	0.00	−0.34	0.00	0.00	0.08	0.00	0.00	0.00	−0.12	0.00
	2	0.00	0.00	−0.03	0.00	0.00	0.00	−0.12	0.00	0.00	−0.01	0.00	0.00	0.00	−0.10
	3	0.00	0.00	0.00	−0.03	0.00	0.00	0.00	0.00	0.00	0.00	0.00	0.00	0.00	0.00

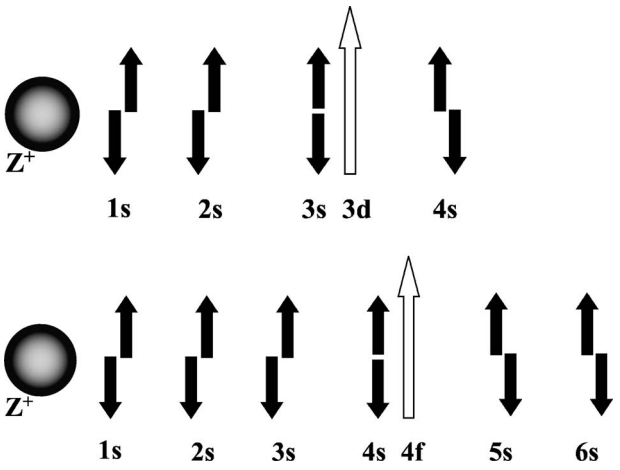

FIG. 11. The core polarization mechanism for 3*d* and 4*f* free ions.

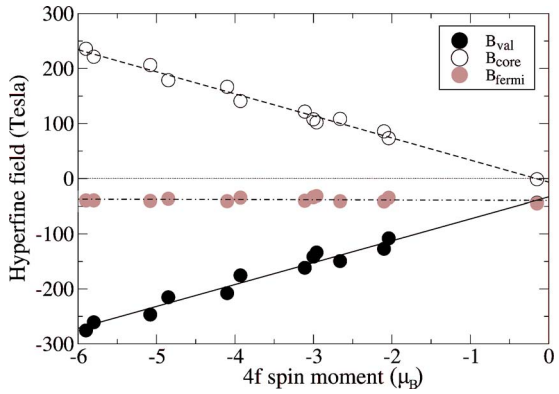

FIG. 12. (Color online) Fermi contact contribution to the HFF as a function of 4*f* spin moment for a large set of different solutions for different lanthanides in Fe. White circles: core contribution (1*s*-4*s*). Black circles: valence contribution (5*s*-6*s*). Gray circles: total Fermi contact contribution. The lines through the core and valence contributions are linear fits; the line through the total Fermi field is the sum of those two fits.

thanides in Fe comes from the fact that in the latter situation the 6*s* electrons will participate in bonding, being insensitive to the 4*f* moment (even for a zero 4*f* moment we have a nonzero 6*s* contribution). As a result the 6*s* contribution to the Fermi HFF is constant through the lanthanide series (Table VII). Moreover, the 5*s* contribution (almost) cancels the 3*s* contribution and what we get as the total Fermi is therefore mainly due to the constant (valence) 6*s* contribution. There is also a $p_{1/2}$ contribution to the Fermi HFF (because in a relativistic treatment the $p_{1/2}$ electrons have also a nonzero probability to be found at the position of the nucleus) mainly coming from the $3p_{1/2}$ electrons, but this contribution is rather small. There is no compelling reason for this observed 3*s*-5*s* cancellation; it is merely a numerical coincidence. But once this coincidence is realized for one lanthanide, it must be there for all of them—which leads to the Fermi field in Fig. 3(c) that is almost independent of the individual lanthanide, a behavior that is strikingly different from the free ion case. The valence, core, and total Fermi fields for lanthanides in Fe are plotted in Fig. 12. It should be noted here that the core part from this calculated Fermi field most likely suffers from the typical "LDA core error," for which recently a promising cure has been proposed.[76] The sum of these three contributions (orbital, dipolar, and Fermi) finally represents the total hyperfine field of trivalent lanthanides in Fe (Fig. 1).

Let us now analyze the evolution of the hyperfine fields obtained with the CDM method, without the crystal field interaction yet. The agreement between the calculated and experimental HFF's is good, especially in the middle of the lanthanides series (Fig. 1, "CDM"). However, there are deviations at the edges. The differences for Er and Tm will be shown later to be due to crystal field effects. For Ce and Pr, we will suggest the delocalization of the 4*f* electrons to play an important role. Only for Yb is there a large deviation between an accurate and reliable experimental value of −125 T (TDPAC) and a calculated value for the 3^+ ion of −467 T. Comparing the experimental results for Yb and Lu, one can see that the HFF's are almost equal. This points to the fact that Yb has the same electronic configuration as Lu, which means that Yb is divalent. It is known that Yb often appears in a divalent configuration, where the 4*f* shell is completely filled. We can calculate such a divalent configuration by using the HOO method and filling the orbitals in a Hund-like way but with one electron more than in the trivalent situation [dashed gray (blue) line in Fig. 1(b)]. This results in the −39 T of the Fermi contact field only, which is in much better agreement with experiment. Nevertheless, a trivalent configuration was suggested before,[43] from the following experimental considerations: the −125 T for Yb in Fe was considered to be "large," much larger than the (−)61 T for the divalent Lu in Fe. This additional −64 T was taken as stemming from an orbital contribution, which must lead to the conclusion that the Yb is trivalent. From Fig. 1(b), however, we see that such a difference of 64 T is almost negligible and that the expected orbital contribution for a trivalent state would be 10 times larger. Another lanthanide that is often divalent is Eu. The bare experimental data in Fig. 1(b) show that there is a sizable difference between the HFF for Eu and for Gd: they must have different electronic configu-

TABLE VII. Individual contributions to the Fermi HFF (in tesla). The $p_{1/2}$ contribution stems mainly from the $3p_{1/2}$ electrons (90%–95%).

	1*s*	2*s*	3*s*	4*s*	5*s*	6*s*	$p_{1/2}$	Total
Tb	0	20	207	−33	−191	−56	14	−39
Er	0	14	129	−30	−106	−57	9	−41
Lu	0	0	−2	0	10	−53	0	−45

rations, and Eu cannot be divalent. This is confirmed by our calculated CDM value for the HFF of Eu^{3+}, which agrees much better than the HOO value for Eu^{2+}. Moreover, Mössbauer isomer shift data[49,50] convincingly point to trivalency for Eu in Fe. We conclude that all lanthanides in Fe are trivalent, except for the divalent Yb. It is somewhat surprising that the valency of Eu and Yb is different.

Finally, we have to discuss the influence of the crystal field. If we compare the HFF's with and without CF effects included (Fig. 3), we notice a few differences. The orbital contribution decreases in the second half when including the CF. On the one hand, this is due to the fact that the CF tends to make the electron distribution over the m orbitals more isotropic (=a larger deviation from integer values in the density matrices). In the first half of the series, the density matrix elements were far from being integer even before including the CF, and therefore the influence of the CF in the first half is much less outspoken. On the other hand, by adding the CF the ground state may change (see Fig. 6 for Yb), a fact which is reflected in the m-orbital occupation. For instance, in the case of Yb the $m=+3$ orbital, which is unoccupied in the absence of the CF, is filled when CF effects are taken into account while the occupation of the $m=+2$ orbital decreases. For Sm the situation is slightly different. While for the other lanthanides the exchange splitting is significantly smaller than the spin-orbit splitting (see Fig. 6 for Ce and Yb), in the case of Sm the exchange and spin-orbit splittings are comparable ($\Delta E_{exc}=403$ K, $\Delta E_{SO}=1184$ K), which causes a mixing of the sublevels with different J. This fact leads to dipolar and Fermi contributions for Sm that are very different from the ones of the neighbors. But again, similar to the case of the other lanthanides, the CF alters the spin density matrices which leads to a different dipolar contribution.

The sum of the three contributions with crystal field included [black (red) solid lines in Fig. 3] gives the total value of the HFF, which is given by the solid black (red) line in Fig. 1(b). The inclusion of CF effects clearly results in a better agreement with experiment, especially for the heavier rare earths. For the lighter rare earths, however, a moderate deviation from experiment remains (Ce to Sm). For Nd and Sm, this is not very significant as the experimental values are not too meaningful (see Sec. III A). But for Pr and especially for Ce (the latter having been measured with the very reliable NMR/ON method), the deviation is undeniable. Can this be explained? Figure 1(b) shows as well that for Ce and Pr the LDA results are much closer to experiment. As was mentioned in Sec. I, LDA calculations for lanthanides represent an itinerant (also called delocalized) $4f$ configuration, which is mostly not what is found in nature: the radius of the $4f$ orbitals is not very large, overlap with the orbitals of neighboring atoms is negligible, and as a result the $4f$ orbitals are localized. The only exception is Ce. As the $4f$ radius gets smaller for increasing atomic number Z, the $4f$ orbitals of Ce reach most outwards. Their radius is large enough to allow overlap and hence delocalization in materials where the nearest-neighbor distance is not too large. Therefore, Ce can be either trivalent or itinerant, depending on the material.[65,77] One can say that in the lanthanide series there is a delocalization-localization transition, which happens already at the very first element Ce. The good agreement between experiments and the LDA results up to Pr in Fig. 1(b) suggests that *for lanthanides in Fe not only Ce but also Pr has delocalized* $4f$ *electrons*: a "postponed" delocalization-localization transition. Two additional arguments support this hypothesis. First, the lanthanide-Fe distance is 2.60 Å, which is considerably smaller than a typical lanthanide-lanthanide distance in pure lanthanide metals (4.08 Å). One can expect from this a large overlap between the $4f$ orbitals and the Fe $3d$, and hence a stronger tendency to delocalization. This argument will be further quantified in terms of pressure in Sec. VI B. We conclude that there are several strong indications that the delocalization-localization transition for lanthanides in Fe is somewhat postponed, at least up to Pr and perhaps further until at most Sm (Eu is certainly localized). We will come back to this in Sec. VI B.

Analyzing the whole set of calculations and experiments for the HFF (Fig. 1), we conclude that the magnitudes of the HFF's with LDA+U are much closer to experiment than with the LDA, certainly for the heavier lanthanides. Together with the ferrimagnetic coupling which is reproduced by LDA+U but not everywhere by the LDA (Fig. 5), this is strong evidence for the fact that LDA+U performs considerably better than the LDA also in these systems.

B. Electric-field gradients

As in an LDA calculation all f orbitals are roughly equally populated, there is almost no spatial anisotropy and V_{zz} will be close to zero (dotted line in Fig. 4). We therefore turn immediately to LDA+U calculations. We are confronted with the same problems as described in Sec. IV B 1. Following the same procedure as for the calculation of the HFF, we use the spin density matrices (spin up, spin down, and cross term) obtained from LANTHANIDE and we calculate V_{zz} for trivalent lanthanides in Fe. Using the procedure leading to the HOO method we determine again the individual contribution to V_{zz} of every $4f$ m orbital and the induced $5p$ contributions to V_{zz} (Fig. 9 and Table V) without considering the cross terms. As in the case of the hyperfine field, these results will be more valid for the heaviest lanthanides. Finally, we include the CF interaction and perform the corresponding constrained density matrix calculations, as was done for the HFF.

Just as for the dipolar HFF, the V_{zz} due to the $4f$ orbitals themselves does not depend on the direction of motion of the electron, and $\pm m$ orbitals yield the same V_{zz}. On the other hand, the V_{zz} depends on the charge and not on the spin, such that also up and down $4f$ electrons yield the same V_{zz}. The $5p$ contribution depends on the $4f$ occupation, just as for the dipolar HFF.

Using the CDM method with crystal field, we obtain reasonable agreement with experiment [Fig. 4, solid black (red) line]. Although there are quite large deviations, the trend of the EFG's is clearly reproduced. In our calculations the EFG's appear to be systematically underestimated. We suggest the following scenario to explain this behavior. It is known that in LDA(+U) the radial part of the $4f$ wave function is too diffuse.[78,79] More specifically, $\langle r^{-3}\rangle$ agrees well with experiment, but $\langle r^{-4}\rangle$ and $\langle r^{-6}\rangle$ are too small. Based on

TABLE VIII. Contributions to V_{zz} for Tb in Fe, with the down channel for Tb $4f$ completely filled and with for the $4f$-up channel one electron in the $m=-1$ orbital. The first column gives the rigorous notation of each contribution (see Ref. 80). In the second column an interpretative notation is defined, which is used in the text and in Fig. 9. The third column gives the energy region in the density of states (DOS) near to which these states are found (E_F means "near the Fermi energy," and negative values are below the Fermi energy). Units: 10^{21} V/m^2.

		In DOS (eV)	Up	Down	
$V_{zz}^{d\text{-}d}$ $(5d)$	V_{zz}^{5d}	E_F	0.1	0.4	
$V_{zz}^{p\text{-}p}$ $(5p)$	V_{zz}^{5p}	−23	5.6	9.6	
$V_{zz}^{p\text{-}p}$ $(6p)$	V_{zz}^{6p}	E_F	−0.2	0.4	
$V_{zz}^{f\text{-}f}$ $(4f)$	V_{zz}^{4f}	−5	−29.0	2.5	
V_{zz}			−23.5	12.9	sum=−10.6

these facts, one could conclude that ($4f$ contributions to the) EFG's for lanthanides should be well reproduced (V_{zz} depends on $\langle r^{-3}\rangle$). We have shown (Fig. 9), however, that there is a substantial $5p$ contribution to V_{zz} as well, and we will in the coming paragraphs elaborate on this point (see also Table VIII). We therefore suggest that the $4f$ contribution to V_{zz} is indeed correct (due to the good $\langle r^{-3}\rangle$), but that the deviations in the $4f$ wave functions as signaled by $\langle r^{-4}\rangle$ and $\langle r^{-6}\rangle$ *slightly* disturb the deformation of the $5p$ orbitals near the nucleus, resulting in an incorrect $5p$ contribution. As we will see soon, even tiny changes in the $5p$ orbitals will generate sizable contributions to the EFG. The underestimation of the EFG's in Fig. 4 can therefore be understood as an indirect manifestation of the too diffuse LDA(+U) $4f$ wave functions.

Figure 4 provides further evidence for the fact that Yb in Fe really is divalent: trivalent Yb has a very large V_{zz}, while the experimental value is zero, in agreement with the divalent prediction obtained from the HOO method (which can be trusted, because Yb is a heavy lanthanide).

Now we can analyze which are the main electrons that provide the anisotropy that leads to the EFG. It has been shown before[80] in a rigorous way that for metals with s, p, and d electrons the total V_{zz} can be obtained as a sum of a quantity $V_{zz}^{p\text{-}p}$ and $V_{zz}^{d\text{-}d}$ (neglecting small contributions from the interstitial region of the crystal). They measure the nonspherical p and d charge densities $\rho_{20}^{p\text{-}p}(r)$ and $\rho_{20}^{d\text{-}d}(r)$, respectively, weighted by an integral over $1/r^3$:

$$V_{zz}^{p\text{-}p} \propto \int_0^R \frac{\rho_{20}^{p\text{-}p}}{r^3} dr, \tag{9}$$

$$V_{zz}^{d\text{-}d} \propto \int_0^R \frac{\rho_{20}^{d\text{-}d}}{r^3} dr. \tag{10}$$

R is the radius of the muffin tin sphere of the considered atom. The factor $1/r^3$ strongly emphasizes the contribution from the region close to the nucleus, with small r. s electrons do not contribute as they have spherical symmetry, and so-called "mixed" s-d or s-p contributions are negligible and therefore omitted. This can be extended to materials with f electrons, such that V_{zz} for lanthanides can be written as

$$V_{zz} \approx V_{zz}^{p\text{-}p} + V_{zz}^{d\text{-}d} + V_{zz}^{f\text{-}f}. \tag{11}$$

We now apply this analysis to Tb in Fe, which is a particularly clear example because all $4f$-down orbitals are fully occupied and there is only a single $4f$-up electron. Table VIII shows the different contributions to V_{zz} when this single electron is put in the $m=-1$ (up) orbital (this is not the ground state, but this is just an example, anyway). Table VIII shows that the main contribution to the total $V_{zz}=-10.6\times10^{21}$ V/m^2 is due to the single $4f$-up electron: $V_{zz}^{4f}=-29.0$. There is a large contribution of 5.6+9.6=15.2 with the opposite sign due to p electrons. What is surprising is that this p contribution does not stem from the valence $6p$ electrons, but from the entirely filled and strongly bound $5p$ shell, which lies more than 20 eV below the Fermi energy. Intuitively, one would have assumed such a filled and well-bound shell to be entirely spherically symmetric, which would mean $V_{zz}^{5p}=0$. And indeed, the $5p$ anisotropy $\Delta p=\frac{1}{2}(n_{p_x}+n_{p_y})-n_{p_z}$ is very small: 0.0030 (up) and 0.0040 (down) (it is shown in Ref. 80 that Δp is proportional to V_{zz}^{5p}; n_{p_i} is the number of electrons in the p_i orbital, and Δp measures the unequal occupation of the three p orbitals). However, a considerable part of this anisotropy stems from a region very close to the nucleus and hence gets amplified by the $1/r^3$ factor. This is demonstrated in Fig. 13, where for the same Tb-configuration the bare anisotropic p-p charge density $\rho_{20}^{p\text{-}p}(r)$ is shown, before [Fig. 13(a)] and after [Fig. 13(b)] weighing with a $1/r$ factor and also after integration [Fig. 13(b), right axis]. Figures 13(c) and 13(d) repeat this for the f-f contribution. The final integrals are clearly determined exclusively by anisotropies in a region closer than 0.05 Å to the nucleus. In the expression for a spin dipolar field, the same factor $1/r^3$ is present, explaining why a similar dependence of the $5p$ dipolar field on the $4f$ occupation was observed there [Figs. 8(c)–8(e)]. The orbital hyperfine field depends on $1/r$, such that contributions from the region where $r\approx0$ are much less enhanced—such an effect is indeed absent in Fig. 7.

A generalization of this analysis for Tb is given in Fig. 9, which shows the same individual $4f$ m orbital contributions to V_{zz} for lanthanides split into $4f$ and $5p$ [i.e., when a given $4f$ m orbital is occupied, Figs. 9(a) and 9(b) show the direct contribution from this orbital, while Fig. 9(e) shows the corresponding induced contribution of the $5p$ shell (up and down summed)]. This shows that the existence of opposite signs for $5p$ and $4f$ as seen in the example of Tb is a general effect: occupying the $4f$ $m=0$ orbital gives a negative direct $4f$ contribution but induces a positive $5p$ contribution, etc. This can be understood as follows. A negative V_{zz} corresponds to charge accumulation along the z axis, a positive V_{zz} to charge accumulation in the xy plane. The shape of the $4f$ orbitals is such that $m=0$ has its charge mainly along the z axis (reflected in a negative V_{zz}^{4f}), while the xy plane is more and more occupied for larger $|m|$. Apparently the $4f$ electrons dispel the $5p$ electrons: if $m=0$ is occupied, then the $5p$ electrons are forced away from the z axis into the xy plane,

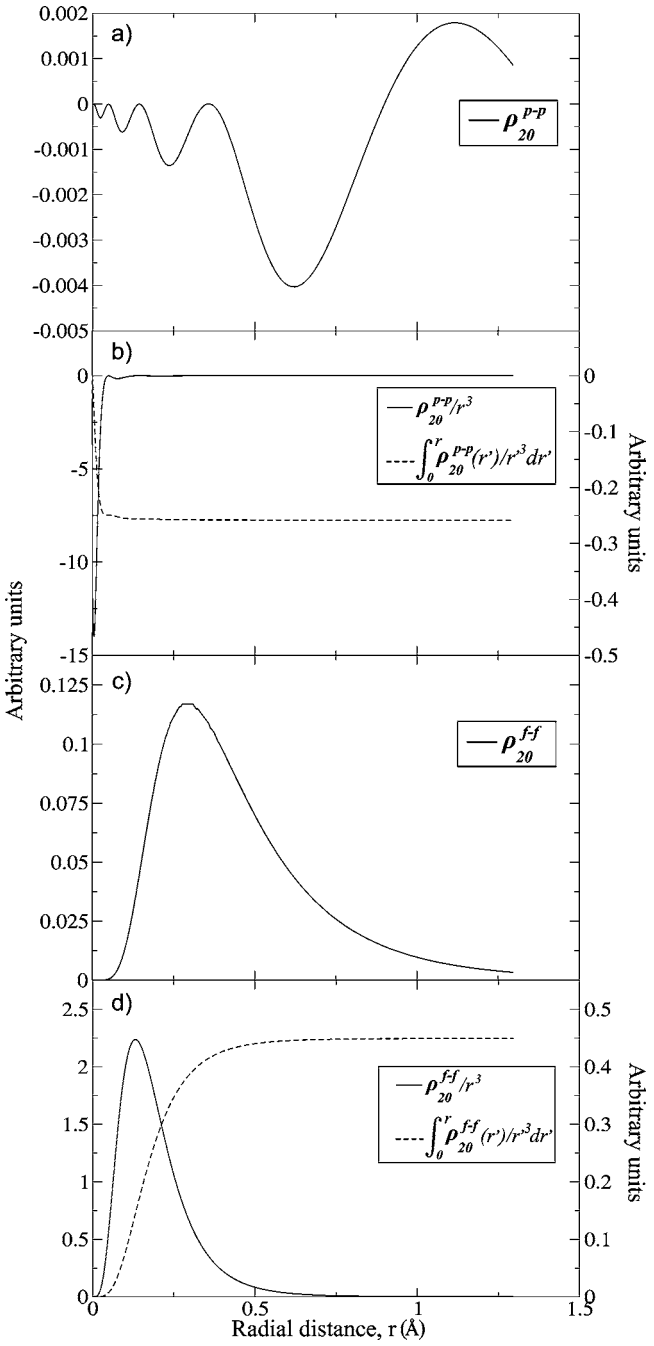

FIG. 13. (a) The anisotropic p density $\rho_{20}^{p\text{-}p}(r)$ for Tb in Fe (sum of up and down electrons, arbitrary units for y scale). (b) Left axis (arbitrary units): $\rho_{20}^{p\text{-}p}(r)/r^3$ for Tb in Fe. Right axis (arbitrary units): integral of $\rho_{20}^{p\text{-}p}(r)/r^3$, which is called $V_{zz}^{p\text{-}p}$ (apart from a constant factor with negative sign). (c) and (d) The same, but for the f-f contribution.

resulting in a positive V_{zz}^{5p} and Δp. As Table VIII shows, a $4f$-up electron distorts the $5p$ orbitals with either spin: this part of the effect is an interaction between the electron charges, not between the spins. But also the spin matters, given the jump at Gd in Fig. 9. This is the effect of the Pauli principle, as mentioned already in Sec. IV B 3: for the light lanthanides, the spin-down channel is being filled (antiparallel alignment with Fe), and these down-electrons repel the $5p$ down in a different way than they do for the $5p$ up.

A similar large $5p$ contribution has been seen for the Gd-EFG in in Gd borocarbide[15] and in $GdCo_5$.[81] However, in those cases the half-filled $4f$ shell is necessarily spherically symmetric and does not contribute to the EFG. Gd is at a noncubic site in those compounds, which results in a strong $6p$ EFG. Such a $6p$ contributions is derived from tails of the wave functions of neighboring atoms. It is therefore the *environment* that induces the $5p$ EFG (interatomic effect). In our case, the lanthanides are at a cubic site (indeed, the $6p$ contribution to the EFG is almost zero) and the $5p$ contribution is induced by the $4f$ electrons of the same atom (intraatomic effect).

Recently, the EFG of the actinide U has been analyzed in UO_2 by Laskowski *et al.* (Ref. 82), using the same APW +lo method as used in this work. These authors show in their Fig. 2 the contributions of $V_{zz}^{p\text{-}p}$, $V_{zz}^{d\text{-}d}$, and $V_{zz}^{f\text{-}f}$ as a function of the deformation of the oxygen cage that surrounds the U atom. They do not further divide the p-p contribution in $6p$ and $7p$ (for actinides it is the $6p$ shell that is entirely filled and well bound). Without deformation of the oxygen cage, the crystallographic surrounding is cubic and the slightly nonzero $V_{zz} \approx -2 \times 10^{21}$ V/m^2 is due to spin-orbit coupling only, as is the case for lanthanides in Fe (compare with Nd in Fig. 4). This small V_{zz} is a sum of a f-f contribution of +20 and a p-p contribution of −21 (the d-d contribution is small: −1). This can be compared to Fig. 9 for Nd with the $m=(-3,-2,-1)$ orbitals filled, which leads to a $4f$ contribution +14 and a $5p$ contribution of −12, quite similar values. Because of this analogy, we suggest that also for U in UO_2 the p-p contribution for an undistorted oxygen cage is due to the completely filled $6p$ shell. This interpretation would, furthermore, imply that as a function of oxygen cage deformation, the $6p$ contribution in Fig. 2 of Ref. 82 would remain almost constant (just as the $5f$ contribution does) and that the strong decrease of the total p-p contribution is due to $7p$ only. This makes sense, as this decrease is attributed[82] to the tails of the O $2p$ wave functions and hence should appear near the Fermi energy (=the region of the $7p$).

VI. ELABORATIONS

A. Temperature dependence

For the effective Hamiltonian (1) as implemented in the LANTHANIDE program, the effect of temperature can be included by occupying the energy levels according to a Boltzmann distribution. In this way we could easily obtain the spin density matrices for a given temperature, and using these matrices for a CDM or HOO calculation, we could find predictions for the HFF and EFG of all lanthanides in the range 0–400 K. The results are not unambiguous, however. The density matrix elements are significantly influenced, by increasing the temperature. The general tendency is that matrix elements that were integer (0 or 1) at 0 K become fractional at elevated temperature. This makes it unlikely that the HOO method produces reliable results, as this method is exact only in the limit of purely integer matrix elements. These unreliable temperature-dependent HFF's found by HOO changed by up to 300 T over the studied temperature range.

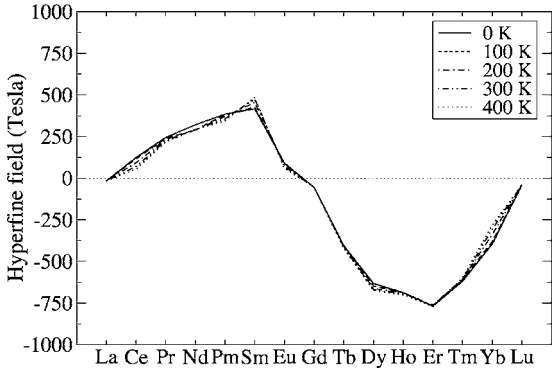

FIG. 14. Total hyperfine field (in tesla) as a function of temperature.

We expected a qualitatively similar behavior when using the more reliable CDM, but remarkably enough the HFF's (and also the EFG's) with CDM where almost identical for all temperatures (Fig. 14). It seems that the effect of the different occupation of the m orbitals (diagonal elements of the density matrix, and the only elements HOO is sensitive to) is almost exactly canceled by the appearence of off-diagonal terms and cross-term contributions at higher temperature. The cancellation seems to be too perfect to be accidental, and we conjecture that this effect has a mathematical origin.

B. Pressure

It is well known experimentally[83] that the pure lanthanides exhibit a large variety of structural phase transitions as a function of external pressure. At certain pressures, volume collapses are sometimes observed and attributed to the delocalization of the f electrons. These delocalization pressures have been determined for six elements of the lanthanide series: Ce,[84,85] Pr,[86–89] Nd,[90–92] Sm,[90,93,94] Gd[83] and Dy[95] (Fig. 15). For Ce the delocalization of the f electrons occurs around the pressure of 1 GPa and is accompanied by a volume collapse of 16% at the isostructural transition to another fcc phase (α-Ce). Pr transforms to a α-U structure at 20 GPa with a volume collapse of 9%–12%. In Gd $4f$ delocalization occurs at 59 GPa when the structure changes to body-centered monoclinic (bcm) with a volume collapse of 10.6% and in Dy this happens at 73 GPa with a volume collapse of 6%. For Nd and Sm no volume collapse has been observed. In these two cases the delocalization of the $4f$ electrons was associated with the appearance of low-symmetry structures (similar with those that appear in Pr, Gd, and Dy cases with volume collapse). This is a somewhat ambiguous procedure. For Nd two transition pressures have been proposed: 40 GPa (corresponding to the transition to an hP3 structure[90,91]) and 113 GPa (corresponding to the transition to the α-U phase[92]). For Sm the delocalization pressure is proposed to be 37 GPa, when the Sm structure changes to hP3. For Pm we have only a lower limit for the transition pressure, 60 GPa (until this pressure no low-symmetry structure has been observed[96]). In our calculations for lanthanide impurities we replace an Fe atom from an iron lattice by a lanthanide atom. Obviously the lanthanide atom (which has a much larger volume) will feel a "chemical" or "effective" pressure. How large will this effective pressure be? We concluded in Sec. V A that at least Ce and Pr are delocalized. Hence, the effective pressure—which we assume to be independent of the lanthanide in a first approximation—should be at least 20 GPa (Fig. 15). The hyperfine fields for Nd and Sm are only very approximately measured [Fig. 1(a)], such that one cannot conclude whether they are localized or not. Based on the isomer shift and EFG (Fig. 4), Eu is definitely localized, as are all heavier lanthanides. Therefore, two qualitatively different proposals for the effective pressure are possible: about 25 GPa (everything starting with Nd is localized) or about 40 GPa (everything below Eu is delocalized, except for Pm and maybe Nd). Assuming an effective pressure that is not constant (motivated by the decreasing volume of heavier lanthanides) does not change this picture (dotted lines in Fig. 15—these lines qualitatively take the lanthanide contraction into account). A more accurate experimental determination of HFF and EFG for Nd, Pm, and Sm in Fe would allow us to distinguish between both scenarios and would allow us to determine the real position of the delocalization-localization transition in this system. Experimental data for Nd in Fe are also for another reason interesting: if Nd in Fe would be found to be localized (itinerant) and the effective pressure of 40 GPa would known to be correct (from a Sm measurement, for instance), then the delocalization pressure of 113 GPa (35 GPa) for bulk Nd is probably correct. If the effective pressure of 25 GPa would be correct, no such conclusion can be made.

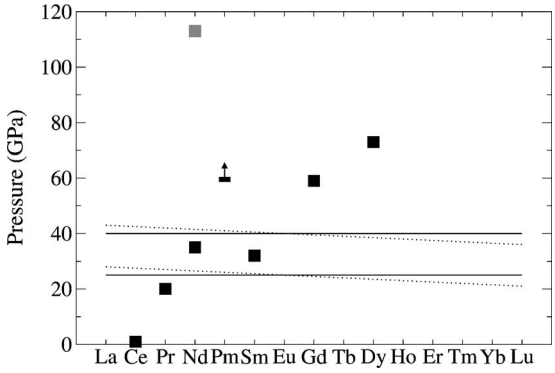

FIG. 15. The experimental transition pressure from localized $4f$ to delocalized $4f$ electrons for pure lanthanides (squares) and two possible choices for the effective pressure felt by lanthanides in Fe (solid and dotted lines) (for details see text).

In conclusion for this section, accurate measurement of HFF and EFG for Nd, Pm, or Sm in Fe would offer a lot of information.

C. Free lanthanide ions

LDA+U calculations for free lanthanide 3^+ ions were already mentioned in Figs. 7–9. A quite complete experimental data set exists for this situation as well, both for the HFF [Fig. 16(a)] and the EFG [Fig. 16(b)] (data are copied from Ref. 97; the original data are in Ref. 98). In the experiments, the ions were not really free but were incorporated in a para-

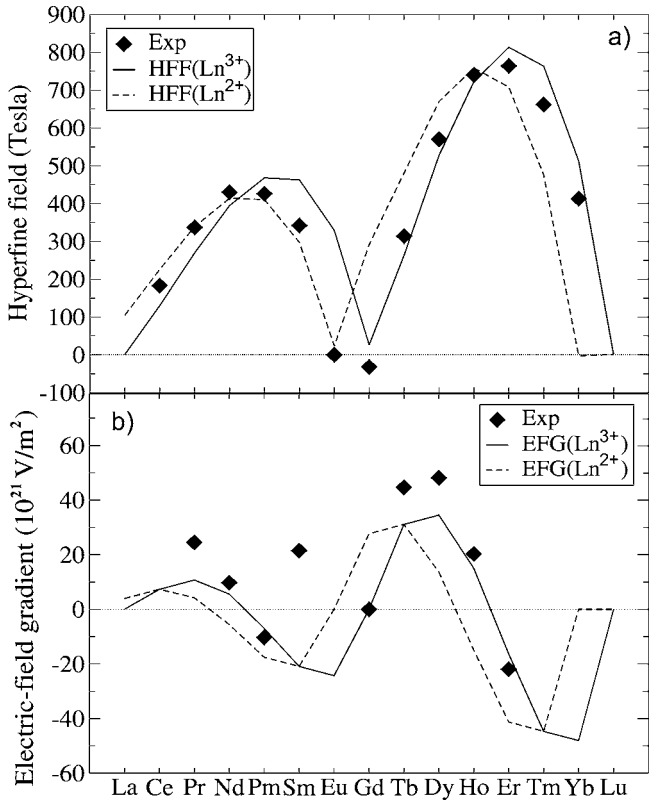

FIG. 16. (a) Experimental value for the HFF in free lanthanide ions, compared with LDA+U predictions based on Figs. 7, 8, and 12 both for divalent and trivalent lanthanides. (b) Experimental value for V_{zz} in free lanthanide ions, compared with LDA+U predictions based on Fig. 9, for both divalent and trivalent lanthanides.

magnetic salt, and the effect of crystal fields was removed later in order to find the free ion values. By the orbitals according to Hund's rules and using the information from Figs. 7–9 we obtained predictions for the HFF and V_{zz} for divalent and trivalent lanthanide ions, which are given by dashed and solid lines in Fig. 16, respectively. For lanthanides in Fe, the positive z direction was naturally defined by the moments of the ferromagnetic Fe host atoms. For free lanthanides, the total (=spin+orbital) angular momentum J determines the positive z direction. Due to this different choice of axes, there is an *apparent* sign change for the heavy lanthanides between Fig. 1 (in Fe) and Fig. 16(a) (free). The agreement with experiment is again quite nice. Eu is divalent (it was trivalent in Fe), while Yb is trivalent (it was divalent in Fe). For Sm there is a large deviation, for both the HFF and V_{zz}. But this is no surprise: it is well known (see also Sec. V A) that there are low-lying excited states in Sm which will mix with the ground state, such that our procedure which is based on Hund's rules ground states is expected to fail.

D. Noncollinear magnetism

The possibility to consider noncollinear magnetism at every infinitesimal region of space has recently been implemented[82] in the WIEN2k code. In principal this can be an important feature even for collinear antiferromagnets as we are dealing with here: it allows the spin moment to turn *gradually* from the Fe orientation to the opposite lanthanide orientation, and this is a better replication of what happens also in nature. We did not attempt a full study, but calculated the HFF and EFG for Tm in Fe only. All technical parameters were chosen exactly the same as in the collinear calculations. For Tm in Fe as a test example, the total HFF changes from −822 T in the collinear LDA+U calculation to −838 T in a noncollinear one, while the EFG remains exactly the same: -38.1×10^{21} V/m^2. Such a change of 16 T is not small in absolute value, but is negligible compared to the large values of the HFF's in this problem. Therefore we conclude that noncollinear magnetism does not play an important role for lanthanides in Fe.

VII. CONCLUSIONS AND OUTLOOK

We have demonstrated that with the LDA+U method a qualitative and quantitative agreement with experiment is obtained for HFF's of lanthanides in Fe. With the LDA the deviation with experiment is much worse and for several cases an incorrect sign of the HFF is predicted. The trend of the EFG's is also well reproduced by LDA+U, the deviations from experiment probably being caused by the 4f wave functions that are rendered too diffuse by LDA-based methods. These results show that the semi *ab initio* LDA+U method is a useful tool, even for such sensitive quantities as the hyperfine parameters of strongly correlated impurities in an itinerant magnetic host. We could come to these conclusions only after applying a careful strategy in order to cope with the lack of a good criterion to determine the true ground state if LDA+U is used: the density matrices for the 4f orbitals were obtained first using a free atom code—specifying the appropriate exchange field and crystal field parameters—and were subsequently kept fixed in the LDA+U calculation (CDM method). We were able to assign quantitative values to the unknown parameters in the single-ion Hamiltonian for lanthanides [Eq. (1)]: the exchange field (420 T) could be determined by requiring a proportionality between the parallel-antiparallel energy difference and the lanthanide spin moment, while the crystal field parameters were found by comparing a large set of HFF's calculated for different crystal field parameters with experiments. As expected, CF effects are important especially at the edges of the lanthanide series. For all lanthanides the 4f spin moment couples ferrimagnetically to the Fe 3d moment, in agreement with the model of Campbell and Brooks. The orbital HFF is by far the dominant contribution to the total HFF (Figs. 1 and 3). We discovered a strong contribution of the completely filled 5p shell to the dipolar HFF and to the EFG, which can be explained by their common $1/r^3$ dependence: small deformations of the 5p shell in a region close to the nucleus are strongly emphasized. A reinterpretation of recent EFG calculations[82] for uranium in UO_2 suggests that the same is true for the 6p shell in actinides. Furthermore, we conclude that Yb is divalent in an Fe host, while all other lanthanides are trivalent (including Eu). The lightest lanthanides (at least up to Pr) show delocalized 4f behavior, and we conclude that

the delocalization-localization transition that typically happens already at Ce is postponed for lanthanides in Fe: it falls at least after Pr and current experiments do not exclude that it could go up to Sm (although Pm is certainly localized). This can be explained by the large effective pressure that is felt by these lanthanide impurities (either 25 or 40 GPa, Fig. 15), leading to a larger overlap between the 4*f* wave functions and the neighboring Fe 3*d*. The question of a postponed localization transition has never been touched on before in the 40 years of experiments on this system. This illustrates what can be the added value of *ab initio* calculations for hyperfine interaction studies. Also in the case of free lanthanide ions, HFF and EFG can be quantitatively reproduced. Remarkably, Eu is divalent in this case and Yb is trivalent—just the opposite as for lanthanides in Fe. The effect of fully noncollinear magnetism on this problem was tested to be negligible.

With the current methods, there are only limited possibilities to improve the accuracy of the calculations. The supercell can be extended to, e.g., 32 atoms and relaxation of the Fe neighbors can be calculated for every individual element (this requires the calculation of forces including spin-orbit coupling and LDA+U, which is time consuming and not yet fully implemented in WIEN2k). But as inevitably a rather arbitrary choice remains to be made for the value of *U*, it is not clear whether these sophistications will really improve the agreement with experiment. And most likely they will not add anything new to the physical insight. In our opinion, new progress in this topic will have to come from experiments. Many of the experimentally determined HFF's and EFG's carry still large error bars. Accurate measurements—for instance, with the NMR/ON method—are desirable (note that NMR/ON has not yet been applied for any of the lanthanides with a large EFG and/or HFF: such large hyperfine interactions put severe requirements on the equipment). The predicted HFF's and EFG's from this work should allow one to reduce considerably the frequency domain that has to be scanned in an NMR/ON experiment and warrants a more physical and reliable interpretation of the observed resonances. As with most worthwhile experiments, we suggest a more accurate determination of HFF and EFG for Pr to Sm: this would allow one to examine experimentally the position of the delocalization-localization transition. Another interesting case is Ho, for which we predict that its HFF is almost a linear interpolation between the values for Dy and Er—about 150 T smaller than what would be expected from a smooth interpolation of the experimental dataset.

Once finally an experimental data set with improved accuracy becomes available, it can serve in its turn as a testing ground for future generations of *ab initio* many-body methods. This work is illustrative for a paradigm shift that is going on in hyperfine interactions studies (and in many other subfields of condensed matter physics): physical insight and hints for what is interesting to measure experimentally are both obtained in the first place by *ab initio* calculations.

ACKNOWLEDGMENTS

Illuminating discussions with P. Blaha (Vienna), P. Novák (Prague), Th. Mazet (Nancy), K. Schwarz (Vienna), M. Diviš (Prague), G. Madsen (Åarhus), S. Blügel (Jülich), J. Mestnik-Filho (São Paulo), B. Barbara (Grenoble), M. Rotter (Vienna), N. Severijns (Leuven), and P. Schuurmans (SCK/CEN-Mol, Belgium) are gratefully acknowledged. We are much indebted to S. Edvardsson and D. Åberg for their willingness to implement a density matrix module into their LANTHANIDE code. The invaluable technical assistance by L. Verwilst, J. Knuts, and P. Mallaerts regarding the computer infrastructure in Leuven is gratefully acknowledged. This work has been performed in the frame of Projects Nos. G.0239.03 and G.0447.05 of the "Fonds voor Wetenschappelijk Onderzoek–Vlaanderen" (FWO), the Concerted Action of the K.U.Leuven (GOA/2004/02), the Centers of Excellence Programme of the K.U.Leuven (INPAC, EF/05/005), and the Inter-University Attraction Pole program (IUAP P5/1).

*Electronic address: Stefaan.Cottenier@fys.kuleuven.be

[1] G. Rao, Hyperfine Interact. **24-26**, 1119 (1985).
[2] H. Akai, M. Akai, S. Blügel, B. Drittler, H. Ebert, K. Terakura, R. Zeller, and P. H. Dederichs, Suppl. Prog. Theor. Phys. **101**, 11 (1990).
[3] H. Haas, Hyperfine Interact. **151/152**, 173 (2003).
[4] H. Akai, M. Akai, S. Blügel, R. Zeller, and P. H. Dederichs, J. Magn. Magn. Mater. **45**, 291 (1984).
[5] M. Akai, H. Akai, and J. Kanamori, J. Phys. Soc. Jpn. **54**, 4246 (1985).
[6] H. Akai, M. Akai, and J. Kanamori, J. Phys. Soc. Jpn. **54**, 4257 (1985).
[7] T. Korhonen, A. Settels, N. Papanikolaou, R. Zeller, and P. H. Dederichs, Phys. Rev. B **62**, 452 (2000).
[8] S. Cottenier and H. Haas, Phys. Rev. B **62**, 461 (2000).
[9] H. Ebert, R. Zeller, B. Drittler, and P. H. Dederichs, J. Appl. Phys. **67**, 4576 (1990).
[10] M. Akai, H. Akai, and J. Kanamori, J. Phys. Soc. Jpn. **56**, 1064 (1987).
[11] M. Takeda, H. Akai, and J. Kanamori, Hyperfine Interact. **78**, 383 (1993).
[12] L. Niesen, Hyperfine Interact. **2**, 15 (1976).
[13] A. L. de Oliveira, N. A. de Oliveira, and A. Troper, J. Phys.: Condens. Matter **14**, 1949 (2002).
[14] M. Richter, J. Phys. D **31**, 1017 (1998).
[15] M. Diviš, K. Schwarz, P. Blaha, G. Hilscher, H. Michor, and S. Khmelevskyi, Phys. Rev. B **62**, 6774 (2000).
[16] L. Petit, A. Svane, Z. Szotek, P. Strange, H. Winer, and W. M. Temmerman, J. Phys.: Condens. Matter **13**, 8697 (2001).
[17] S. J. Asadabadi, S. Cottenier, H. Akbarzadeh, R. Saki, and M. Rots, Phys. Rev. B **66**, 195103 (2002).
[18] V. I. Anisimov and O. Gunnarsson, Phys. Rev. B **43**, 7570 (1991).
[19] M. T. Czyżyk and G. A. Sawatzky, Phys. Rev. B **49**, 14211

(1994).
[20] V. I. Anisimov, I. V. Solovyev, M. A. Korotin, M. T. Czyżyk, and G. A. Sawatzky, Phys. Rev. B **48**, 16929 (1993).
[21] A. G. Petukhov, I. I. Mazin, L. Chioncel, and A. I. Lichtenstein, Phys. Rev. B **67**, 153106 (2003).
[22] V. I. Anisimov, F. Aryasetiawan, and A. I. Lichtenstein, J. Phys.: Condens. Matter **9**, 767 (1997).
[23] V. N. Antonov, B. N. Harmon, and A. N. Yaresko, Phys. Rev. B **66**, 165208 (2002).
[24] R. Laskowski, P. Blaha, and K. Schwarz, Phys. Rev. B **67**, 075102 (2003).
[25] D. W. Boukhvalov, V. V. Dobrovitski, M. I. Katsnelson, A. I. Lichtenstein, B. N. Harmon, and P. Kogerler, J. Appl. Phys. **93**, 7080 (2003).
[26] A. B. Shick and O. N. Mryasov, Phys. Rev. B **67**, 172407 (2003).
[27] G. Seewald, E. Hagn, E. Zech, D. Forkel-Wirth, A. Burchard, and the ISOLDE Collaboration, Phys. Rev. Lett. **78**, 1795 (1997).
[28] G. Seewald, E. Hagn, E. Zech, R. Kleyna, M. Voss, D. Forkel-Wirth, A. Burchard, and the ISOLDE Collaboration, Phys. Rev. Lett. **82**, 1024 (1999).
[29] G. Seewald, E. Hagn, E. Zech, R. Kleyna, M. Voss, A. Burchard, and the ISOLDE Collaboration, Phys. Rev. B **66**, 174401 (2002).
[30] P. Hohenberg and W. Kohn, Phys. Rev. **136**, B864 (1964).
[31] W. Kohn and L. J. Sham, Phys. Rev. **140**, A1133 (1965).
[32] S. Cottenier, *Density Functional Theory and the family of (L)APW-methods: a step-by-step introduction* (Instituut voor Kern-en Stralingsfysica, K. U. Leuven, Belgium) (freely available at http://www.wien2k.at/reg_user/textbooks).
[33] E. Sjöstedt, L. Nordström, and D. J. Singh, Solid State Commun. **114**, 15 (2000).
[34] G. K. H. Madsen, P. Blaha, K. Schwarz, E. Sjöstedt, and L. Nordström, Phys. Rev. B **64**, 195134 (2001).
[35] P. Blaha, K. Schwarz, G. Madsen, D. Kvasnicka, and J. Luitz, computer code WIEN2k, an augmented plane wave+local orbitals program for calculating crystal properties, Karlheinz Schwarz, Technische Universität Wien, Austria, 1999.
[36] J. P. Perdew and Y. Wang, Phys. Rev. B **45**, 13244 (1992).
[37] S. Blügel, H. Akai, R. Zeller, and P. H. Dederichs, Phys. Rev. B **35**, 3271 (1987).
[38] J. Kuneš, P. Novák, R. Schmid, P. Blaha, and K. Schwarz, Phys. Rev. B **64**, 153102 (2001).
[39] D. D. Koelling and B. N. Harmon, J. Phys. C **10**, 3107 (1977).
[40] J. Goto, M. Tanigaki, A. Taniguchi, Y. Ohkubo, Y. Kawase, S. Ohya, K. Nishimura, T. Ohtsubo, and S. Muto, J. Phys. Soc. Jpn. **72**, 723 (2003).
[41] W. van Rijswijk, F. van den Berg, W. Joosten, and W. Huiskamp, Hyperfine Interact. **15/16**, 325 (1983).
[42] P. Herzog, U. Dämmrich, K. Freitag, C.-D. Herrmann, and K. Schlösse, Hyperfine Interact. **22**, 167 (1985).
[43] H. Devare, H. de Waard, and L. Niesen, Hyperfine Interact. **5**, 191 (1978).
[44] O. Klepper, H. Spehl, and N. Wertz, Z. Phys. **217**, 425 (1968).
[45] G. Russel, private communication to D. A. Shirley, cited in T. A. Koster and D. A. Shirley, in *Proceedings of the International Conference on Hyperfine Interactions in Excited Nuclei*, edited by G. Goldring and R. Kalish (Gordon and Breach, London 1971), p. 1239.
[46] F. Boehm, G. Hagemann, and A. Winther, Phys. Lett. **21**, 217 (1966).
[47] L. Grodzins, R. Borchers, and G. Hagemann, Phys. Lett. **21**, 214 (1966).
[48] R. Brenn, L. Lehmann, and H. Spehl, Z. Phys. **209**, 197 (1968).
[49] R. Cohen, G. Beyer, and B. Deutch, Phys. Rev. Lett. **33**, 518 (1974).
[50] L. Niesen and S. Ofer, Hyperfine Interact. **4**, 347 (1978).
[51] H. Wit, L. Niesen, and H. D. Waard, Hyperfine Interact. **5**, 233 (1978).
[52] L. Niesen, P. Kikkert, and H. D. Waard, Hyperfine Interact. **3**, 109 (1977).
[53] P. G. E. Reid, N. J. Stone, H. Bernas, D. Spanjaard, and I. Campbell, Proc. R. Soc. London, Ser. A **311**, 169 (1969).
[54] L. Niesen, Ph.D. thesis, University of Leiden, 1971.
[55] H. W. Kugel, T. Polga, R. Kalish, and R. R. Borchers, in *Hyperfine Interactions in Excited Nuclei*, edited by G. Goldring and R. Kalish (Gordon and Breach, New York, 1971), p. 104.
[56] H. W. Kugel, L. Eytel, G. Hubler, and D. E. Murnick, Phys. Rev. B **13**, 3697 (1976).
[57] H. Bernas and H. Gabriel, Phys. Rev. B **7**, 468 (1973).
[58] I. Campbell, J. Phys. F: Met. Phys. **2**, L47 (1972).
[59] M. Brooks, O. Eriksson, and B. Johansson, J. Phys.: Condens. Matter **1**, 5861 (1989).
[60] W. van Rijswijk, F. van den Berg, H. E. Keus, and W. J. Huiskamp, Physica B & C **113**, 127 (1982).
[61] E. Fermi, Z. Phys. **60**, 320 (1930).
[62] M. Liebs, K. Hummler, and M. Fähnle, Phys. Rev. B **46**, 11201 (1992).
[63] B. N. Harmon, V. Antropov, A. I. Liechtenstein, I. V. Solovyev, and V. I. Anisimov, J. Phys. Chem. Solids **56**, 1521 (1995).
[64] J. F. Herbst, R. E. Watson, and J. W. Wilkins, Phys. Rev. B **17**, 3089 (1978).
[65] B. I. Min, H. Jansen, T. Oguchi, and A. J. Freeman, J. Magn. Magn. Mater. **61**, 139 (1986).
[66] A. B. Shick, A. I. Liechtenstein, and W. E. Pickett, Phys. Rev. B **60**, 10763 (1999).
[67] H. Eschrig, K. Koepernik, and I. Chaplygin, J. Solid State Chem. **176**, 482 (2003).
[68] J. Kuneš, H. Rosner, D. Kasinathan, C. O. Rodriguez, and W. E. Pickett, Phys. Rev. B **68**, 115101 (2003).
[69] S. Edvardsson and D. Åberg, Comput. Phys. Commun. **133**, 396 (2001).
[70] D. Torumba, Ph.D thesis (unpublished).
[71] M. Rotter, J. Magn. Magn. Mater. **90**, 272 (2004).
[72] W. T. Carnall, G. L. Goodman, K. Rajnak, and R. S. Rana, J. Chem. Phys. **90**, 3443 (1989).
[73] B. G. Wybourne, *Spectroscopic Properties of Rare Earths* (Interscience, New York, 1965).
[74] A. J. Freeman and R. E. Watson, in *Magnetism*, edited by G. T. Rado (Academic Press, New York, 1965), p. 167.
[75] R. E. Watson and A. J. Freeman, Phys. Rev. **123**, 2027 (1961).
[76] P. Novák, J. Kuneš, W. E. Pickett, W. Ku, and F. R. Wagner, Phys. Rev. B **67**, 140403(R) (2003).
[77] J. L. Smith, Z. Fisk, and S. S. Hecker, Physica B & C **130**, 151 (1985).
[78] J. Forstreuter, L. Steinbeck, M. Richter, and H. Eschrig, Phys. Rev. B **55**, 9415 (1997).
[79] M. Richter, in *Handbook of Magnetic Materials*, edited by K. H. J. Buschow (Elsevier Science, Amsterdam, 2001), Vol. 13.
[80] P. Blaha, K. Schwarz, and P. H. Dederichs, Phys. Rev. B **37**, 2792 (1988).

[81] G. H. O. Daalderop, P. J. Kelly, and M. F. H. Schuurmans, Phys. Rev. B **53**, 14415 (1996).
[82] R. Laskowski, G. K. H. Madsen, P. Blaha, and K. Schwarz, Phys. Rev. B **69**, 140408(R) (2004).
[83] A. K. McMahan, C. Huscroft, R. T. Scalettar, and E. L. Pollock, J. Comput.-Aided Mater. Des. **5**, 131 (1998).
[84] W. H. Zachariasen and F. H. Ellinger, Acta Crystallogr., Sect. A: Cryst. Phys., Diffr., Theor. Gen. Crystallogr. **33**, 155 (1977).
[85] J. S. Olsen, L. Gerward, U. Benedict, and J.-P. Itié, Physica B **133**, 129 (1985).
[86] G. S. Smith and J. Akella, J. Appl. Phys. **53**, 9212 (1982).
[87] W. A. Grosshans, Y. K. Vohra, and W. B. Holzapfel, J. Phys. F: Met. Phys. **13**, L147 (1983).
[88] Y. C. Zhao, F. Porsch, and W. B. Holzapfel, Phys. Rev. B **52**, 134 (1995).
[89] B. J. Baer, H. Cynn, V. Iota, C.-S. Yoo, and G. Shen, Phys. Rev. B **67**, 134115 (2003).
[90] Y. C. Zhao, F. Porsch, and W. B. Holzapfel, Phys. Rev. B **50**, 6603 (1994).
[91] J. Akella, S. T. Weir, Y. K. Vohra, H. Prokop, S. A. Catledge, and G. N. Chesnut, J. Phys.: Condens. Matter **11**, 6515 (1999).
[92] G. N. Chesnut and Y. K. Vohra, Phys. Rev. B **61**, R3768 (2000).
[93] W. A. Grosshans and W. B. Holzapfel, J. Phys. (Paris) **45**, 141 (1984).
[94] J. S. Olsen, S. Steenstrup, L. Gerward, U. Benedict, J. Akella, and G. Smith, High Press. Res. **4**, 366 (1990).
[95] R. Patterson, C. K. Saw, and J. Akella, J. Appl. Phys. **95**, 5443 (2004).
[96] R. G. Haire, S. Heathman, and U. Benedict, High Press. Res. **2**, 273 (1990).
[97] W. D. Brewer, Hyperfine Interact. **59**, 201 (1990).
[98] B. Bleaney, in *Magnetic Properties of the Rare-Earth Metals*, edited by R. Elliot (Plenum Press, London, 1972), p. 383.